# DISTRIBUTED ACTIVE VIBRATION CONTROL WITH EMBEDDED SENSOR NETWORK TECHNIQUES

By

Tao Tao

Dissertation

Submitted to the Faculty of the

Graduate School of Vanderbilt University

in partial fulfillment of the requirements

for the degree of

DOCTOR OF PHILOSOPHY

in

Electrical Engineering

August, 2006

Nashville, Tennessee

Approved:

Professor Kenneth D. Frampton

Professor Gautam Biswas

Professor George E. Cook

Professor Nilanjan Sarkar

Professor D. Mitchell Wilkes

TABLE OF CONTENTS

# ACKNOWLEDGEMENTS

First and foremost, I thank my advisor, Dr. Kenneth D. Frampton, for his guidance, teaching, support, and friendship. I truly appreciate all the time and efforts he devoted to my research, personal growth, and career development during my study at Vanderbilt University. His work spirit of being an original researcher, critical evaluator to research results, and open-minded learner will impact my career for the rest of my life.

I would also like to thank my other committee members for their helpful insights and contributions: Dr. George Cook, Dr. Gautam Biswas, Dr. D. Mitchell Wilkes and Dr. Nilanjan Sarkar.

I thank all members in our research group for their help: Peter Schmidt, Isaac Amundson and Chakradhar R. Byreddy. I especially thank Peter and Isaac for proofreading of my publications, and helping me about my English communicating skills.

I also appreciate the love and support from my parents and my sister all the time. Finally, a special thanks to my wife Niya. I could not have done this without your support.

LIST OF TABLES

LIST OF FIGURES

# CHAPTER I

# INTRODUCTION AND SUMMARY

## Introduction to Vibration Control

Structural vibration control is a very important issue in aerospace engineering and structural engineering. Various vibration control methods have been studied, and these strategies can be categorized into two groups: passive vibration control and active vibration control.

In passive vibration control, passive elements are used to change the system damping and stiffness in order to reduce structural vibration. Although no power source is needed, the dynamics of the plant is often changed, and the weight of the whole system is often increased which is not acceptable in aerospace applications. Furthermore, the structural vibration is only reduced in certain frequency ranges with passive vibration control.

Due to the limitation of passive vibration control, active vibration control was introduced and there has been a great deal of interest in the active vibration control of structures. In order to optimize the control results, additional power is introduced to the system in active vibration control. The structures of active vibration control, with many actuators and sensors, have been made possible by the use of piezoelectric ceramic and piezopolymer film materials as the sensing and actuating devices. Active vibration control is capable of performing over a broad range of operating conditions, and has the advantage of reduced weight over passive damping methods[1].

## Previous Work

There has been a lot of research in the field of active vibration control. One of the earliest works in the field of active vibration and acoustic control was published by Fuller[2]. Feed-forward control was used to reduce narrow band acoustic radiation with structural actuators, and considerable noise attenuations were achieved with this approach[3,4]. Swigert and Forward used PZT as the active damper to control the mechanical vibration of an end-supported mast[5]. Bailey and Hubbard developed the active vibration control system for a cantilever beam using Poly Vinylidence Flouride (PVDF)[6]. St-Amant and Cheng used a FIR controller based on LMS to control the vibration of a plate[7]. Choi performed vibration control with multi-step Bang-Bang control[8]. Baumann and Eure used feedback control to reduce stochastic disturbances such as turbulent boundary layer noise[9,10].

Although active control has been used to reduce structural vibrations for many years[2,11,12], the application of active vibration control on large-scale systems has achieved little success due to the scalability limitations of traditional centralized control architectures. In centralized control, one controller processes all sensor data to generate optimal actuator inputs in order to reduce the structural vibrations. Thus, there is an overwhelming, even impractical, computational burden on the centralized controller, when large-scale systems are considered. Recent advances in Micro-Electro-Mechanical systems (MEMS) and embedded system technologies have enabled the applications of distributed control designs[13], which is more scalable compared with centralized control and suitable for large-scale systems.

A distributed control system normally consists of numerous localized controllers called nodes. Each localized controller has a sensor, an actuator and a means of communicating with other controllers in the system[14,15,16,17,18]. The goal of distributed control systems is to achieve a global performance by sharing sensor information among the localized controllers. This is in contrast to decentralized control whose localized controllers work independently to achieve a global performance[19,20,21,22,23]. Distributed control has been studied for over 30 years, but most of these studies were concerned with "weakly connected" systems, where each local controller only experiences a few of the degrees of freedom of the entire system (e.g. robotic swarms). Recently, distributed control has been studied for noise radiation reduction and vibration reduction[16,24,25,26] which requires control design approaches suitable for strongly connected systems. While these efforts have demonstrated the suitability and scalability of distributed architectures, their performance has not been demonstrated experimentally.

One of the most important, enabling technologies for distributed control systems is distributed middleware. Middleware is software that operates between the operating system and the application (the control law in this case)[27,28]. There are numerous middleware services that would be important to the deployment of a distributed control system. These include network discovery; clock synchronization; distributed resource allocation; network communications routing; and many others. The service that would most affect the performance of distributed control is group management and the inter-node communications that it provides[29,30,31]. Group management services manage the formation and organization of groups of nodes; provide for the communication among nodes; maintain routing Tables; execute leader election and group consensus

applications; clock synchronization; and many other tasks. The reason that group management services are important to distributed control is that they offer the means by which scalable distributed control architectures can be constructed.

Scalability in a distributed control system is very important to its success. This is because as a distributed control system becomes larger the number of nodes increases, resulting in an exponential increase in network communication traffic. However, the ability of the network to transmit this information does not scale up as quickly as the volume of information. Therefore, in order to be scalable the amount of information transmitted must be limited. This can be achieved by forming nodes into groups, and limiting inter-node communications to within those groups. Therefore, by designing control laws that depend only on sensor information from within the group (instead of from all sensors), the network traffic can be limited and the scalability of the system can be ensured. Since these group management services provide scalable communications they provide a promising framework for the current work: that is to develop distributed control algorithms which utilize groups of sensors. While some investigations have been undertaken to include specific models of middleware[32,33] the middleware itself is not included in the simulations presented here. Rather, their existence has served as the framework for designing control systems that take advantage of their capabilities.

The purpose of this work is to investigate distributed control on a non-weakly connected system and to compare sensor grouping techniques that will result in scalable distributed control architectures.

**Decentralized Control with Networked Embedded System**

In this work, a distributed vibration control system is implemented using embedded Prometheus processor boards and a Local Area Network (LAN). Important distributed middleware services required by distributed control systems, such as clock synchronization and network communications routing, were investigated and implemented experimentally.

A simply supported beam was built, and Lead Zirconate Titanate (PZT) patches were attached on the beam acting as sensors and actuators, as shown in Figure 2-2.

The Prometheus boards, from Diamond Systems Corporation, were used as the microprocessor nodes for this research. Each board is a high-integration PC/104 100MHz CPU with a 10/100BaseT Fast Ethernet port, which provides up to 100Mbps network connectivity. A router connects all PC104 nodes, and a local area network (LAN) was established. Each node has a unique IP address in the LAN, and can send and receive data to and from each other via the TCP/IP protocol. The extensive data acquisition circuitry, including analog input channels, analog output channels, digital I/O channels, external triggers, and counters/timers, makes it convenient to connect the embedded controller directly to the sensors and actuators. The detailed specifications of the data acquisition circuit are listed in Table 2-2.

Five piezoceramic actuators were attached to the beam surface. The disturbance to the beam was generated through one of the actuators, and the other four served as control actuators. The location of the actuator generating a disturbance to the beam was chosen to be 0.563m (the distance from the left end of the beam to the center of the actuator), and the other four were placed at the same locations as the sensors. The

voltage from the D/A circuit in the microcontroller was amplified through a power amplifier, and the amplified control voltage drove the control actuators.

When the decentralized control system is running, clocks on all nodes (including the one that only generates the disturbance) will first be synchronized. The clock synchronization was accomplished using Reference Broadcast Synchronization as follows[34]: each node obtains IP addresses of its neighboring nodes, then waits; a packet is broadcast to all nodes in the network; when the packet reaches the physical port of a node, the microprocessor begins to work. Since the nondeterministic processing of TCP and IP layers are not involved in the synchronization procedure, the time taken for a packet to be transported is very small and the synchronization has very high precision of within 10 μs of error.

After the clock synchronization, each microprocessor will generate system interrupts periodically. During the interval, which is 1/600 sec for all nodes, user interrupt routines will run. The four sensor nodes will perform the following steps during the interrupt interval: acquire data from the sensor through the A/D circuit; send the data to the node on its immediate right; receive data from the node on its immediate left; calculate the control voltage using the local data and the data from its left-hand neighbor; and send the control voltage to the actuator through the D/A circuit. The node on the leftmost end of the beam only sends but does not receive data, and the control voltage will be calculated based on its own data. Similarly, the node at the rightmost end of the beam only receives but does not send data. In our experimental setup, the voltage from the D/A circuit is filtered through a low-pass filter with a cutoff frequency of 600 Hz in order to minimize the sensor noise at the accelerometer.

Different clock synchronization methods were investigated on the embedded systems in the LAN, and the Reference Broadcasting Algorithm was chosen and proved effective for distributed vibration control system.

The performance of distributed control system was evaluated by comparison of open-loop and closed-loop system responses in the frequency range of 0-250 Hz. The reduction of the first six natural vibration modes were shown in Figure 2-4.

It is shown that distributed control has better performance than traditional centralized control, and services provided by distributed middleware are critical to implement distributed control.

## Distributed Active Vibration Control

The application of distributed vibration control in the first topic was extended here both analytically and experimentally. The purpose is to investigate the effectiveness of a more robust distributed controller design based on $H_2$ optimal theory and system identification technique. A simply supported beam is chosen as the illustrative flexible structure. A distributed control architecture is designed based on a system identification model and is used to minimize vibration due to broadband disturbances. Experimental results are presented for the control of the beam's vibration modes under 600 Hz.

This work focuses on the vibrations in the range of 0-600 Hz which includes the first nine modes. In order to obtain the most accurate system model from which controllers were designed a system identification approach was used. When the vibration displacements of the beam are small, a linear model can reasonably represent the system. Four sensors and four actuators were used for the control system resulting in sixteen

transfer functions from the inputs to outputs. In addition, the path between disturbance and sensors was also identified. Band-limited white noise was applied to each actuator and sensor data was collected from each sensor. This data was used to get the Auto-Regression with eXtra inputs (ARX) model.

A batch least squares solution was used to find the desired ARX parameters, and a multi-input multi-output (MIMO) state space model was then derived from the ARX model. In order to choose an appropriate system order and obtain the optimal system model, the frequency responses of all signal paths were measured and system identification was performed. The final order of the identified model was chosen to be 36, since it provided the best fit with the lowest order. In Figures 3-3 and 3-4, the transfer functions measured directly from system identification data are depicted with solid lines, and the transfer functions derived from the corresponding state-space model were shown with dotted lines. As shown, the state space model represents the beam dynamics very well, in both magnitude and phase of the system response. The discrepancy at the low frequency range (0-20 Hz) is due to the effect of environmental noise on the response measurements. All other system transfer functions compared similarly well. Furthermore, the frequency peaks of the identified model occur at 8.7, 29.3, 61.0, 105.9, 165.4, 235.8, 318.9, 413.3, and 515.4 Hz. These values compare very well with the theoretical values discussed earlier.

The distributed controller design in this section is based on centralized $H_2$ optimal control theory which has been proven effective at attenuating structural vibration. The centralized $H_2$ optimal controller is extended here to control vibrations under a distributed architecture. In the distributed control architecture each node shared instantaneous sensor

signals with the nodes on either side. In this manner each nodes local compensator used its own sensor signal, as well as those communicated from the two neighboring nodes, to construct the local actuator signal. Thus, two of the local compensators are three-input single-output control system. However, the leftmost and rightmost compensators were two-input single-output. Such an architecture could easily be extended to larger scale systems as has been demonstrated analytically.

In order to fairly compare the performance of these three controllers, the global control efforts were tuned to be equal. As discussed previously, each compensator design was checked to ensure equal control effort based on simulations using the identified model. Furthermore, the control effort was checked experimentally by computing the total control signal power in each case (for equal disturbance power). When experimental discrepancies in control effort were found the compensator was redesigned and the control effort was checked again.

As shown in Figure 3-7, the centralized controller has the best performance, the decentralized controller has the worst performance, and the performance of the distributed controller falls in between. This comparison holds for all of the modal peaks as well as the total vibration power reductions shown in Table 3-1. These results compare well with previous analytical distributed control results, decentralized results, and centralized results.

In comparison to the decentralized controller whose control signals are based only on local sensors, the distributed controller takes advantage of more sensor data including the local sensor, and a better overall control performance is demonstrated. Compared

with the centralized controller, there is less computation when each actuator force is calculated since not all sensor data are needed for each actuator.

It is shown in Table 3-1 that the distributed control architecture presented here approaches the performance of a traditional centralized controller employing the same control effort. In addition, in comparison to centralized control, the distributed controller has the advantages of scalability for application in large systems and that it will continue to perform even when some processors fail, although probably with diminished capability.

## Sensor Groupings for Distributed Vibration Control

In this paper the performance of a distributed vibration control system based on various sensor grouping schemes is demonstrated. The benefit of using sensor groups is that the result control architecture is scalable for use in large-scale systems. A simply supported beam is chosen as the illustrative flexible structure, and two types of sensor grouping strategies are considered: groups based on physical proximity and groups based on modal sensitivity. The global control objective is to minimize the beam's vibrational response under 600 Hz with a performance that approaches that of traditional centralized control.

As described previously, in order to create a distributed control system each localized controller shares sensor information within a group of other controllers in the distributed control architecture. Then, each localized controller is designed according to the sensor data that is available to it using the $H_2$ control design described previously. Therefore, each local controller is locally optimal, but the global system is not optimal.

In order for such an architecture to be scalable (i.e. able to be functional in systems with numerous sensors) the groups must contain only a fraction of the total sensors in the system. One way to achieve this is to organize the sensors based on close physical proximity. Such groups are referred to here as geographic groups and the group size is defined by a groups "reach." The reach of a localized controller is defined as the number of sensors to a particular controllers right and left (plus its own sensor) that are available to it for control implementation. For example, in a distributed control system of reach 1, each local compensator is designed based on its own sensor signal, the signal from the sensor to its left, and the signal from the sensor to its right. Thus, the local subsystems are three-input single-output control system with the exception of the leftmost and rightmost compensators, which are two-input single-output systems.

The transfer function plots are shown in Figure 4-7 for the open loop system and distributed control systems with reach 1, 2 and 3 (i.e. group sizes of 1, 5 and 6 sensors). As shown in Figure 4-7, all distributed systems achieve good vibration reductions, especially on the three dominant vibrational modes: 165.4Hz, 235.8Hz and 318.9Hz. Furthermore, as one would expect, the control performance improves when the reach is increased. As the reach increased, the distributed control architecture approaches the centralized control system since each compensator has most (if not all in the case of some controllers with reach 3) of the system sensor signals available. One would, therefore, expect that the performance of distributed control would approach that of centralized systems. This is demonstrated in Figure 4-8. As shown in Figure 4-8, the distributed control system of reach 3 approaches the performance of a centralized control system at the three dominant vibrational modes. A tentative conclusion based on this result[16] is

that, as the reach of a geographic distributed controller increases and the available sensor signals span a significant amount of the structures length, the performance of the distributed control system will approach that of a centralized controller. This result can be achieved without including all system sensor signals, but only enough to span a significant portion of the length[16].

The performance of a distributed controller of reach 3 was compared to a controller of reach 0 in Figure 4-9. A reach zero controller is equivalent to a decentralized controller since it only utilizes the local sensor signal to create the local control signal. As demonstrated by Figure 4-9 distributed control significantly outperforms the decentralized compensator at the three dominant vibration frequencies. Vibrational modes at the lower frequency range are also reduced further when compared to decentralized control system. The advantage of a purely decentralized control system is that it is infinitely scalable. That is to say, as the number of system sensors increases there is no increase in controller complexity since there is no communication among separate localized controllers. However, the advantage of a distributed controller is that it's performance is better than decentralized, but at the cost of added complexity both in terms of signal communications and controller complexity. But, when applied to a large scale system, the trade off between performance and complexity offered by a distributed system, as compared to either decentralized or centralized, offers system designers some choices.

In distributed control system based on modal grouping strategy, a group contain a fixed number of localized controllers that posses the highest sensitivity to the vibrational mode to be targeted by that group. Three dominant vibrational modes are targeted for

attenuation: 163 Hz, 234 Hz and 320 Hz. Therefore, three groups are formed each containing 3 sensors. The sensitivity of each sensor to each mode is determined by the frequency response magnitude of that specific signal path. The sensitivities of each sensor are shown in Table 4-2 and the grouping is shown in Table 4-3. In the group targeting the $7^{th}$ vibrational mode sensor 5 is included even though it is not among the top three transducers sensitive to the mode, so that all transducers in the whole system will be used in the distributed system.

The performance of controllers using groups based on modal sensitivity is shown in Figure 4-10 as compared to the reach 1 geographic group architecture. While the modal group architecture is able to significantly attenuate the three target modes, it achieves less attenuation than the reach 1 geographic architecture. Both of these architectures employ groups with 3 members each. A similar result was noted based on computer simulations[16]. This result is unexpected since modal based control systems have proven effective in previous investigations. It may be true that with larger group sizes and optimized sensor grouping, that this trend would not continue.

A final comparison of all control architecture's overall performance is provided in Table 4-4, which shows the total H2-norm between the disturbance input and all sensor outputs. Note that, as stated previously, centralized control offers the best performance overall. However, among distributed control architectures the geographic groups offer the best performance when compared to the modal groups.

It is shown that distributed control has a better performance than decentralized control, and the performance can be improved by increasing the reach or number of sensors in a group. Experimental results demonstrate that the distributed control method

approaches the performance of a traditional centralized controller when as the size of the group is increased. A further advantage of these group-based architectures is that they are scalable for use in large scale systems, similar to the decentralized design.

## Fault-Tolerant Active Vibration Control

A fault-tolerant active vibration control system is applied to a simply supported beam with high order in this topic. System failures are detected and isolated by Beard-Jones (BJ) filters, and then a controller specifically designed for the faulty system is switched on, in order to maintain optimal control performance and stability under failure conditions.

Since sensors and actuators are normally involved in such active control systems, the implementation of Fault Detection and Isolation (FDI) for sensor or actuator failures have been investigated for long-term safety[35,36,37,38,39]. However, no work has been done in fault-tolerant vibration control, since the high order vibration system limits the application of traditional fault-tolerant strategies. Another limitation is that there are no existing design techniques than can accommodate a model with feed-through dynamics (i.e. a state space model with non-zero D matrix). The vibration system models are normally obtained with system identification techniques, which usually result in models with feed-through dynamics[40,41,42].

In this work, the performance of a fault-tolerant active vibration control system is demonstrated experimentally. The fault tolerant method in this paper is based on BJ filters, and applicable for high order systems with feed-through dynamics. A simply supported beam with three pairs of piezoelectric transducers acting as sensors and

actuators is the active structure investigated. The basic theory of BJ filters is summarized, and then followed by the development of two modifications to existing feedback matrix design techniques. The first modification enables BJ filters to be designed for systems with feed-through dynamics while the second modification presents a gain matrix design suitable for high order systems.

The failure of an actuator was implemented by unplugging the BNC cable from the Digital Analog Converter (DAC) on the dSPACE connection panel. And the time history of continuous residual, discrete residual, finite state and the output of sensor 2 were presented in Figure 7. It is shown that where there is a failure at actuator 2 around 38 seconds, the BJ filter detects the failure and the discrete residual is set to be 1 for actuator 2. The value of finite state is 3, which represents the failure of actuator 2 and switches the controller. Although the performance of the controller is a little worse after switch, the closed-loop system is stable and the transition between controller switch is negligible.

The results of the experiment with two actuator failures are shown in Figures 5-8, 5-9 and 5-10. The failure of actuator 2 happened around 40 seconds, and the failure of actuator 1 took place around 60 seconds. The continuous residuals for both actuators are shown in Figure 5-8, and the BJ filter in our system detected both failures well. The discrete residuals and finite state for actuators 1 & 2 failures are shown in Figure 5-9. When actuator 2 failed around 40 seconds, the discrete residual for actuator 2 was changed to 1, and the finite state was set to be 3, which switched the controller to the specific one in the controller library. Then, when actuator 1 failed around 60 seconds, the discrete residual for actuator 1 was changed to 1, and the finite state was set to be 4 and

the controller was switched again. The corresponding sensor signals are shown in Figure 5-10.

The transfer functions from the disturbance to sensor 1 in different fault situations are shown in Figure 5-11. It is shown that the system with no actuator failures has the best control performance, but the closed-loop system in our system is stable and fault-tolerant, even the control performance is compromised.

## References


[1] S. M. Kuo and D. R. Morgan, "Active noise control: a tutorial review," Proceedings of the IEEE, Vol. 87, No. 6, 1999, pp. 943-975.

[2] C. R. Fuller, "Experiments on reduction of aircraft interior noise using active control of fuselage vibration," Journal of the Acoustical Society of America, Vol. 78, No. S1, 1985, pp. S88.

[3] R. L. Clark and D. E. Cox, "Multi-variable structural acoustic control with static compensation," Journal of the Acoustical Society of America, Vol. 102, No. 5, 1997, pp. 2747-2756.

[4] R. L. Clark and C. R. Fuller, "Experiments on active control of structurally radiated sound using multiple piezoceramic actuators," Journal of the Acoustical Society of America, Vol. 91, No. 6, 1992, pp. 3313-3320.

[5] C. J. Swigert and R. L. Forward, "Electronic damping of orthogonal bending modes in a cylindrical mast - theory," Journal of Spacecraft and Rockets, Vol. 18, No. 1, 1981, pp. 5-10.

[6] T. Bailey and J. E. Hubbard, "Distributed piezoelectric polymer active vibration control of a cantilever beam," Journal of Guidance Control and Dynamics, Vol. 8, No. 5, 1985, pp. 605-611.

[7] Y. St-Amant and L. Cheng, "Simulations and experiments on active vibration control of a plate with integrated piezoceramics," Thin-Walled Structures, Vol. 38, No. 2, 2000, pp. 105-123.

[8] S. B. Choi, "Alleviation of Chattering in Flexible Beam Control Via Piezofilm Actuator and Sensor," Aiaa Journal, Vol. 33, No. 3, 1995, pp. 564-567.

[9] W. T. Baumann, "An adaptive feedback approach to structural vibration suppression," Journal of Sound and Vibration, Vol. 205, No. 1, 1997, pp. 121-133.

[10] K. W. Eure, "Adaptive predictive feedback techniques for vibration control," in *Electrical Engineering*. Blacksburg, VA: Virginia Polytechnic Institute and State University, 1998.

[11] W. T. Baumann, W. R. Saunders, and H. H. Robertshaw, "Active suppression of acoustic radiation from impulsively excited structures," Journal of the Acoustical Society of America, Vol. 90, No. 6, 1991, pp. 3202-3208.

[12] R. L. Clark and C. R. Fuller, "Control of sound radiation with adaptive structures," Journal of Intelligent Material Systems and Structures, Vol. 2, No. 3, 1991, pp. 431-452.

[13] C. Y. Chong and S. P. Kumar, "Sensor networks: evolution, opportunities, and challenges," Proceedings of the IEEE, Vol. 91, No. 8, 2003, pp. 1247-1256.

[14] S. Burke and J. Hubbard, Jr., "Active vibration control of a simply supported beam using a spatially distributed actuator," IEEE Control Systems Magazine, Vol. 7, No. 4, 1987, pp. 25-30.

[15] R. S. Chandra, J. Fowler, and R. D'Andrea, "Control of interconnected systems of finite spatial extent," IEEE Conference on Decision and Control, No., 2002, pp. 238-239.

[16] K. D. Frampton, "Distributed group-based vibration control with a networked embedded system," Smart Materials & Structures, Vol. 14, No. 2, 2005, pp. 307-314.

[17] B. Sinopoli, C. Sharp, L. Schenato, S. Schaffert, and S. S. Sastry, "Distributed control applications within sensor networks," Proceedings of the IEEE, Vol. 91, No. 8, 2003, pp. 1235-1246.

[18] E. Scholte and R. D'Andrea, "Active vibro-acoustic control of a flexible beam using distributed control," American Control Conference, Denver, CO, 2003.

[19] G. West-Vukovich, E. Davison, and P. Hughes, "The decentralized control of large flexible space structures," IEEE Transactions on Automatic Control, Vol. 29, No. 10, 1984, pp. 866-879.

[20] K. D. Frampton, "Decentralized control of structural acoustic radiation," Proceedings of IMECE 2000, New York, NY, 2001.

[21] M. Baudry, P. Micheau, and A. Berry, "Decentralized harmonic active vibration control of a flexible plate using piezoelectric actuator-sensor pairs," Journal of the Acoustical Society of America, Vol. 119, No. 1, 2006, pp. 262-277.

[22] O. N. Baumann, W. P. Engels, and S. J. Elliott, "A comparison of centralized and decentralized control for the reduction of kinetic energy and radiated sound power," Proceedings of Active04, Williamsburg, VA, 2004.

[23] M. J. Brennan, S. J. Elliott, and X. Huang, "A demonstration of active vibration isolation using decentralized velocity feedback control," Smart Materials & Structures, Vol. 15, No. 1, 2006, pp. N19-N22.

[24] W. P. Engels, O. N. Baumann, S. J. Elliott, and R. Fraanje, "Centralized and decentralized control of structural vibration and sound radiation," Journal of the Acoustical Society of America, Vol. 119, No. 3, 2006, pp. 1487-1495.

[25] P. Gardonio, E. Bianchi, and S. J. Elliott, "Smart panel with multiple decentralized units for the control of sound transmission. Part I: theoretical predictions," Journal of Sound and Vibration, Vol. 274, No. 1-2, 2004, pp. 163-192.

[26] P. Gardonio, E. Bianchi, and S. J. Elliott, "Smart panel with multiple decentralized units for the control of sound transmission. Part II: design of the decentralized control units," Journal of Sound and Vibration, Vol. 274, No. 1-2, 2004, pp. 193-213.

[27] N. A. Lynch, *Distributed Algorithms*, Morgan Kaufmann Publishers, 1996.

[28] D. C. Schmidt and S. D. Huston, *C++ Network Programming: Mastering Complexity Using ACE and Patterns*, Addison-Wesley Longman, 2002.

[29] R. Nagpal and D. Coore, "An algorithm for group formation in an amorphous computer," Proceedings of the 10th International Conference on Parallel and Distributed Computing Systems (PDCS'98), Nevada, October 1998.

[30] G.-C. Roman, Q. Huang, and A. Hazem, "Consistent group membership in ad hoc networks," Proceedings of the 23rd International Conference on Software Engineering (ICSE), 2001.

[31] R. Vitenberg, I. Keidar, and G. V. Chockler, "Group communication specifications: a comprehensive study," ACM Computing Surveys, Vol. 33, No. 4, December 2001, pp. 1-43.

[32] M. Maroti, K. D. Frampton, G. Karsai, S. Bartok, and A. Ledeczi, "Experimental platform for studying distributed embedded control applications," Proceedings of Languages, Compilers, and Tools for Embedded Systems Conference, Berlin, Germany, June 2002.

[33] T. Tao, K. D. Frampton, and A. Ledeczi, "Simulations of decentralized vibration control with a networked embedded system," Proceedings of SPIE Annual International Symposium on Smart Structures and Materials - The Internation Society for Optical Engineering, San Diego, CA, 2003.

[34] J. Elson, L. Girod, and D. Estrin, "Fine-grained network time synchronization using reference broadcasts," Proceedings of the Fifth Symposium on Operating Systems Design and Implementation, Boston, MA, 2002.

[35] H. Jones, "Failure detection in linear systems," The Charles Stark Draper Laboratory, Cambridge, MA Report No. T-608, 1973.

[36] R. V. Beard, "Failure accommodation in linear systems through self-reorganization," in *Aeronautics and Astronautics*. MA: Massachusetts Institute of Technology, 1971.

[37] J. Chen, R. J. Patton, and H. Y. Zhang, "Design of unknown input observers and robust fault detection filters," International Journal of Control, Vol. 63, No. 1, 1996, pp. 85-105.

[38] Y. Kim and J. Park, "An analysis of detection spaces using invariant zeros," American Control Conference, San Diego, CA, USA, 1999.

[39] R. Scattolini and N. Cattane, "Detection of sensor faults in a large flexible structure," Iee Proceedings-Control Theory and Applications, Vol. 146, No. 5, 1999, pp. 383-388.

[40] R. L. Clark, W. R. Saunders, and G. P. Gibbs, *Adaptive Structures: Dynamics and Control*, Wiley, New York, 1998.

[41] J.-N. Juang, *Applied System Identification*, Prentice Hall, Englewood Cliffs, NJ, 1994.

[42] L. Ljung, *System Identification: Theory for the User*, Prentice Hall, Upper Saddle River, NJ, 1998.

# CHAPTER II

## MANUSCRIPT 1

## DECENTRALIZED VIBRATION CONTROL WITH NETWORKED EMBEDDED SYSTEMS

Tao Tao, Isaac Amundson, and Kenneth D. Frampton

Vanderbilt University

Nashville, TN 37235

(Proceedings of IMECE 2004)

### Abstract

The early promise of centralized active control technologies to improve the performance of large scale, complex systems has not been realized largely due to the inability of centralized control systems to “scale up”; that is, the inability to continue to perform well when the number of sensors and actuators becomes large. Now, recent advances in Micro-electro-mechanical systems (MEMS), microprocessor developments and the breakthroughs in embedded systems technologies, decentralized control systems may see these promises through. A networked embedded system consists of many nodes that possess limited computational capability, sensors, actuators and the ability to communicate with each other over a network. The aim of this decentralized control system is to control the vibration of a structure by using such an embedded system

backbone. The key attributes of such control architectures are that they be scalable and that they be effective within the constraints of embedded systems. Toward this end, the decentralized vibration control of a simply supported beam has been implemented experimentally. The experiments demonstrate that the reduction of the system vibration is realized with the decentralized control strategy while meeting the embedded system constraints, such as a minimum of inter-node sensor data communication, robustness to delays in sensor data and scalability.

## Introduction

The vibration of structures is a very important problem in mechanical engineering, structural engineering, and especially aerospace engineering. There has been a great deal of interest in vibration control of structures in the past decades, and most methods can be categorized into the following two strategies: the attenuation of the noise source, and the attenuation of the noise at the reception location. Passive vibration control, which uses passive elements to change the system damping and stiffness, has been widely used. Although no power source is needed in passive vibration control, the weight of the whole system is often increased which is not acceptable in aerospace applications.

Due to the limitations of passive vibration control, active vibration control was introduced. Most active control designs rest on the presupposition of centrality: one digital computer is used to process the data from all sensors and generate the control forces in order to implement the control algorithm. Centralized control technology is applicable to small and medium sized systems. However, when a large-scale system is

considered, it is very difficult for one computer to meet the overwhelming need for processing efforts. Therefore, there is a trend toward decentralized control for increased reliability and better processing performance. A decentralized control system consists of many embedded microprocessors, sensors and actuators. Depending on the information from the local sensor, a microprocessor will implement some control strategy and generate a control force through an actuator. There has been extensive research on the application of active materials to the vibration control of flexible structures. Swigert and Forward used lead zirconate titanate (PZT) as the active damper to control the mechanical vibration of an end-supported mast[1]. Bailey and Hubbard developed the active vibration control system for a cantilever beam using Poly Vinylidene Flouride (PVDF)[2]. Amant and Cheng used a FIR controller based on LMS to control the vibration of a plate[3]. Choi performed vibration control with multi-step Bang-Bang control[4].

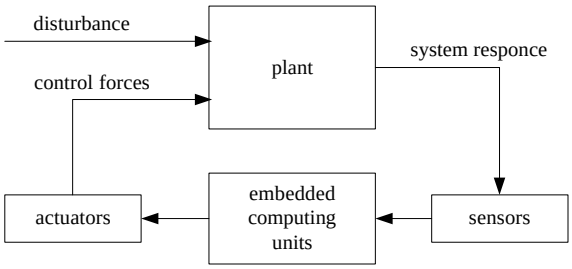


Figure 2-1: Concept of decentralized control

For embedded control systems, the microprocessors used are usually restricted by the available space and power supply, and the control forces are calculated only from the local sensor information. The technological advances of embedded systems and reduced cost of MEMS devices make it possible to realize decentralized control systems in which

the local control force is calculated according to the information not only from its local sensor but also from neighboring sensors as well. A model of such decentralized control systems is illustrated in Figure 2-1.

Decentralized control systems consist of many nodes, each including a computing unit, a sensor and an actuator. All nodes can communicate with each other, so that a node can send its local sensor data to other nodes and receive sensor data from other nodes[5]. When the control system is running, every node in the system will first communicate with each other and calculate its own location, so that a networked embedded system is established. Some disturbance will then cause the plant to vibrate, and the sensors will measure the system response. Each node will send its local sensor data to some specific group of nodes, which is predetermined by the chosen communication configuration. Then the computing unit in each node will implement some control algorithm, such as LQR control, according to its local sensor data and sensor data received from other nodes. The actuators will apply control forces on the plant to complete the feedback control structure.

## Modeling of Physical System

In order to reduce the vibration of structures using decentralized control, it is necessary to have knowledge of the system dynamics. For active vibration control, the physical system includes not only the structure, such as beam and plate structures, but also sensor and actuator devices. Therefore the dynamics of sensor and actuator devices should be considered in order to achieve successful controller design.

**Piezoelectric Actuators**

Many different active transduction materials have been used in various fields, such as shape memory alloy (SMA). However, the most commonly used transduction material is piezoelectric material, and it has been used widely for active vibration control systems.

Piezoelectric materials have some important characteristics: direct piezoelectric effect and inverse piezoelectric effect. When the piezoelectric material has an external load applied, it becomes electrically polarized. Thus, an electrical charge is produced at the surface of the material. This phenomenon is called direct piezoelectric effect, which is utilized for the design of piezoelectric sensors. Conversely, when a voltage is applied to a piezoelectric material, it will induce a strain in the material. This phenomenon is called inverse piezoelectric effect, which is utilized for the design of piezoelectric actuators. Since the direct and inverse piezoelectric effects are designed to be linear over the range of the application, it is very convenient to measure the change of electric field or mechanical load.

Some example piezoelectric materials are natural quartz crystals, polycrystalline piezoceramic and semicrystalline polyvinylidene polymer. The most commonly used piezoelectric materials are usually made from two materials: PZT and PVDF. Different piezoelectric materials have different characteristics, so it is very important to choose an appropriate material. Since a simply supported aluminum beam is the structure considered in this experiment, small patches of PZT are attached to the beam surface and used as the actuators. In order to get maximum control forces from the PZT actuators,

the actuator patches are driven in couples by the voltage, which is demonstrated in Figure 2-2[6].


Figure 2-2: PZT actuators driven in couples

Pairs of PZT actuators are attached to both sides of the beam at the same horizontal locations. When a drive voltage is connected to the PZT pairs in the way shown in Figure 2-2, these two actuators have opposite deformation. For example, the extension of the upper actuator and the contraction of the lower actuator will cause the beam structure to bend more than with only one actuator in place.

**Modeling of a Simply Supported Beam**

The vibrating structure under consideration is a simply supported beam, which is modeled using Galerkin's technique:

$$0 = EI\nabla^4 w(x,t) + rh\frac{\partial^2 w(x,t)}{\partial t^2} + f_d(x,t) + \sum_{k=1}^{K} f_c(x,t) \qquad (1)$$

where $w$(x,t), E, I, ? and h are the beam displacement, modulus of elasticity, moment of inertia, density and thickness, respectively. The beam is acted upon by a disturbance force, $f_d$, and control forces, $f_c$.

The mode shape of the simply supported beam is described as:

$$\Psi_n(x) = \sin\left(\frac{np}{l}x\right) \qquad (2)$$

A separable solution is assumed using the *in vacuuo* beam eigenfunctions and generalized coordinates of the form

$$w(x,t)=\sum_{n=1}^{N}\Psi_n(x)q_n(t)=\sum_{n=1}^{N}\sin(\tfrac{npx}{L})q_n(t) \tag{3}$$

where $q_n(t)$ are the generalized coordinates. Substituting Eq. (3) into Eq. (1), multiplying by an arbitrary expansion function, $?_r(x,y)$, and integrating over the domain yields a set of ordinary differential equations of the form[7]:

$$0=M_s\ddot{q}_n(t)+K_sq_n(t)+\sum_{k=1}^{N}Q_{kn}^{c}(t)+Q_n^{d}(t) \tag{4}$$

where $M_s$ and $K_s$ are the modal mass and stiffness and $Q_{kn}^{c}$ and $Q_n^{d}$ are the control generalized forces and the disturbance generalized forces.

The mass matrix for the beam system is derived as follows:

$$\begin{aligned}M_s(p,q)&=\int_0^l\int_0^w\int_0^h\Psi_r^T(x)r_s(x)\Psi_r(x)dxdydz\\&=rwh\int_0^l\sin\left(\frac{pp}{l}x\right)\sin\left(\frac{qp}{l}x\right)dx\\&=\begin{cases}\dfrac{rlwh}{2} & when\ p=q\\ 0 & when\ p\neq q\end{cases}\end{aligned} \tag{5}$$

The stiffness matrix for the beam system is expressed as:

$$K_s(p,q)=\begin{cases}\dfrac{pEh^3wp^4}{24l^3} & when\ p=q\\ 0 & when\ p\neq q\end{cases} \tag{6}$$

Equation (4) can be cast into state space form[8]:

$$\begin{cases}\dot{x}=Ax+Bu\\ y=Cx+Du\end{cases} \tag{7}$$

The state vector is described as:

$$x = \begin{bmatrix} r & \dot{r} \end{bmatrix}^T \tag{8}$$

where r is the vector of generalized mechanical coordinates.

The input vector consists of disturbance and control forces at all actuators:

$$u = \begin{bmatrix} F_{disturbance} & F_1 & F_2 & \dots & F_{50} \end{bmatrix}^T \tag{9}$$

The matrix A can be expressed as:

$$A = \begin{bmatrix} 0 & I \\ -[M_s]^{-1} K_s & -2x\sqrt{[M_s]^{-1} K_s} \end{bmatrix} \tag{10}$$

where proportional damping has been added to each mode in the above equation.

The matrix B for the simulated beam is expressed as:

$$B = \begin{bmatrix} 0 & 0 \\ I & [Ms]^{-1}\Theta \end{bmatrix} \tag{11}$$

where the coupling matrix is defined as:

$$\Theta = \begin{bmatrix} \sin(1 \times l_1 \times p) & \sin(1 \times l_2 \times p) & \cdots & \sin(1 \times l_k \times p) \\ \sin(2 \times l_1 \times p) & \sin(1 \times l_2 \times p) & \cdots & \sin(1 \times l_k \times p) \\ \vdots & \vdots & \vdots & \vdots \end{bmatrix} \tag{12}$$

and $l_k$ are the coordinates of actuators along the beam.

The matrices C and D depend on the choice of observed outputs, and can be modified to observe any set of variables desired. The matrix D is usually a zero matrix.

Since digital microprocessors are used in the decentralized control systems, the continuous state space equations need to be transformed to discrete-time state space equations:

$$\begin{cases} x_{k+1} = Gx_k + Hu_k \\ y_k = Cx_k + Du_k \end{cases} \tag{13}$$

## Decentralized Control System Design

There are a lot of different strategies to design a stable control system[9], and the design of the control systems in this simulation is based on quadratic performance indexes. For an active vibration control system, the system dynamics can be expressed in state space equations:

$$\dot{x}(t) = Ax(t) + Bu(t) \tag{14}$$

$$y(t) = Cx(t) \tag{15}$$

where x is the state vector, u is the control vector, y is the output vector, and A, B, C are system matrices.

The objective of control system design is to minimize the performance index by choosing the control vector u(t). The standard infinite time quadratic performance index is defined as follows[10]:

$$J = \frac{1}{2}\int_0^\infty \left[x'(t)Qx(t) + u'(t)Ru(t)\right]dt \tag{16}$$

where J is the performance index, Q is a positive-definite (or positive-semidefinite) Hermitian or real symmetric matrix, and R is a positive-definite Hermitian or real symmetric matrix.

The control vector u(t) usually depends on the output vector y(t), and the relationship between the output vector and control vector can be expressed as:

$$u(t) = -Ky(t) \tag{17}$$

where K is the feedback gain matrix.

From previous equations, it is shown that the performance index J is related to the feedback gain matrix. In order to optimize the performance of control systems, the optimal feedback gain matrix should be chosen to minimize the performance index. The

algorithm for computing the optimal feedback gain matrix was first presented in the article by Levine[11].

From Eq. (14), (15) and (17), the state space equation for the system can be rewritten as:

$$\dot{x}(t) = [A - BKC]x(t) \tag{18}$$

The state vector x(t) can be expressed as:

$$x(t) = \Phi(t)x(0) \tag{19}$$

where $\Phi(t)$ is the fundamental transition matrix for the system, and it is defined as:

$$\Phi(t) = e^{([A-BKC]t)} \tag{20}$$

Substituting Eq. (18) and (19) into Eq. (16), the performance index can be rewritten as:

$$J = x'(0)\left[\frac{1}{2}\int_0^\infty \Phi'(t)\left(Q + C'K'RKC\right)\Phi(t)dt\right]x(0) \tag{21}$$

It is shown in Eq. (21) that the performance index depends both on the feedback gain matrix K and the initial state x(0). The initial state x(0) cannot be controlled, and it can be assumed to be a random variable which uniformly distributes on the surface of the dimensional unit sphere. By averaging performance indexes with independent initial states, the initial state x(0) can be eliminated from Eq. (21). Accordingly, in order to optimize the performance and minimize the performance index, we just need to consider the feedback gain matrix K.

From Eq. (21), the following equation can be derived [11]:

$$K_{n-1} = R^{-1}B'F_{n-1}L_{n-1}C'\left[CL_{n-1}C'\right]^{-1} \tag{22}$$

where $F_{n-1}$ is the solution of

$$F_{n-1}[A-BK_{n-2}C]+[A-BK_{n-2}C]^{'}F_{n-1}+Q+C^{'}K_{n-2}^{'}RK_{n-2}C=0 \tag{23}$$

and $L_{n-1}$ is the solution of

$$L_{n-1}[A-BK_{n-2}C]^{'}+[A-BK_{n-2}C]L_{n-1}+I=0 \tag{24}$$

With Eq. (22), (23) and (24), we can obtain the optimal feedback gain matrix K, which makes the control system stable. In order to get the optimal feedback gain for a known system, the first step is guessing an initial value $K_0$ for K, then according to Eq. (23) and (24), $F_1$ and $L_1$ can be calculated. Substituting $F_1$ and $L_1$ into Eq. (22), we can get $K_1$. If the control performance with feedback gain $K_1$ is good enough, then $K_1$ is the expected optimal feedback gain matrix. Otherwise, $K_1$ is used as the initial value to obtain $K_2$, $K_3\ldots$ until the expected control performance is achieved.

The strategy described above has been demonstrated satisfactorily and is used in this simulation to get the optimal feedback gain.

## Experimental Implementations

The verification of distributed vibration control was performed with a simply supported beam shown in Figure 2-3. The experimental setup consists of six major functioning units: a beam, sensors, anti-aliasing circuits, microprocessors, amplifiers and actuators.

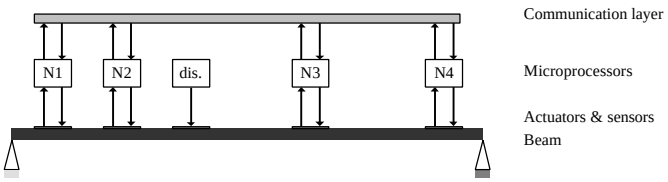


Figure 2-3: Decentralized vibration control of a simply supported beam

The physical properties of the flexible aluminum beam are given in Table 2-1. The beam was machined with knife-edges near the ends to provide the pinned supports.

Table 2-1: Physical properties of the beam

| Parameters | Value |
|---|---|
| Young's Modulus $E$ | 73.1 GPa |
| Density $r$ | 2770 kg/m$^3$ |
| Length $L$ | 1 m |
| Width $b$ | 5.08e-2 m |
| Thickness $h$ | 3.175e-3m |

The vibration of the beam was measured by four accelerometers attached to the beam surface. In order to optimize the control performance, the placement of the sensors should be considered. Sensors were not evenly distributed along the beam. The actual locations of the sensors were 0.125m, 0.25m, 0.688m and 0.875m (the distance from the left end of the beam to the centers of the sensors).

The data acquired at each sensor was filtered and amplified through a circuit board before being transmitted to the corresponding microprocessor. Since the vibrating structure is controlled in the frequency range of between 0-250Hz in these experiments, the cutoff frequency of the $2^{nd}$ order Chebyshev anti-aliasing filter is set to 250Hz in order to minimize the aliasing effect. Although there is an internal amplifier in the accelerometer, the voltage readout representing the structure vibration at each sensor was still small (in the milli-volt range). The filtered data was amplified appropriately, so that the measuring range of the A/D circuit in the microprocessor could be utilized and the measuring resolution improved correspondingly.

Table 2-2: Specifications of the Prometheus data acquisition circuit

| Analog Inputs | |
|---|---|
| Number of inputs | 16 single-ended or 8 differential (user selectable) |
| A/D resolution | 16 bits (1/65536 of full scale) |
| Bipolar ranges | ±10V, ±5V, ±2.5V, ±1.25V (software selectable) |
| Conversion rate | 100,000 samples per second with interrupts |
| Analog Outputs | |
| Number of outputs | 4 lines, Simultaneous update |
| D/A resolution | 12 bits (1/4096 of full scale) |
| Output ranges | Fixed: ±10V, 0-10V (Programmable possible) |

The Prometheus boards from Diamond Systems Corporation were used as the microprocessor nodes for this research. Each board is a high-integration PC/104 100MHz CPU with a 10/100BaseT Fast Ethernet port, which provides up to 100Mbps network connectivity. A router connects all PC104 nodes, and a local area network (LAN) was established. Each node has a unique IP address in the LAN, and can send and receive data to and from each other via the TCP/IP protocol. The extensive data acquisition circuitry, including analog input channels, analog output channels, digital I/O channels, external triggers, and counters/timers, makes it convenient to connect the embedded controller directly to the sensors and actuators. The detailed specifications of the data acquisition circuit are listed in Table 2-2.

Five piezoceramic actuators were attached to the beam surface. The disturbance to the beam was generated through one of the actuators, and the other four served as control actuators. The placement of the actuators should also be considered just as the locations of sensors. The location of the actuator generating a disturbance to the beam was chosen to be 0.563m (the distance from the left end of the beam to the center of the actuator), and the other four were placed at the same locations as the sensors. The voltage from the D/A circuit in the microcontroller was amplified through a power amplifier, and the amplified control voltage drove the control actuators.

The system identification of the structure was performed before the design of the controller. Since we are only interested in the frequency range 0-250Hz, white noise with a frequency range 0-250Hz was generated to excite the structure. The sensor outputs were acquired at the sampling frequency 600Hz. By comparing the measured frequency response of the structure and theoretical FEA model, it was shown that resonant peaks

matched well. This means that the boundary conditions, mass and stiffness of the beam are well simulated. However, some elements in the FE model had to be adjusted to reflect the effect of the electric circuits, sensors and actuators.

After the model of the structure was obtained, the controller was designed using the LQR algorithm described above. The distributed control system could then be implemented. When the decentralized control system is running, clocks on all nodes (including the one that only generates the disturbance) will first be synchronized. The clock synchronization was accomplished using Reference Broadcast Synchronization as follows[12]: each node obtains IP addresses of its neighboring nodes, then waits; a packet is broadcast to all nodes in the network; when the packet reaches the physical port of a node, the microprocessor begins to work. Since the nondeterministic processing of TCP and IP layers are not involved in the synchronization procedure, the time taken for a packet to be transported is very small and the synchronization has very high precision of within 10 μs of error.

After the clock synchronization, each microprocessor will generate system interrupts periodically. During the interval, which is 1/600 sec for all nodes, user interrupt routines will run. The four sensor nodes will perform the following steps during the interrupt interval: acquire data from the sensor through the A/D circuit; send the data to the node on its immediate right; receive data from the node on its immediate left; calculate the control voltage using the local data and the data from its left-hand neighbor; and send the control voltage to the actuator through the D/A circuit. The node on the leftmost end of the beam only sends but does not receive data, and the control voltage will be calculated based on its own data. Similarly, the node at the rightmost end of the

beam only receives but does not send data. In our experimental setup, the voltage from the D/A circuit is filtered through a low-pass filter with a cutoff frequency of 600Hz in order to minimize the sensor noise at the accelerometer.

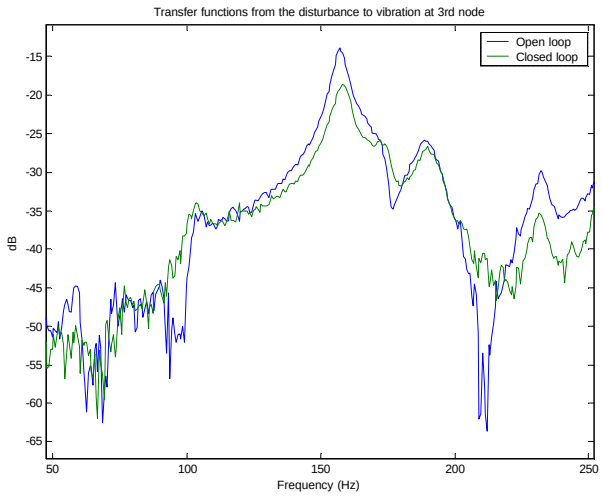


Figure 2-4: Transfer functions of open-loop system and closed-loop system

The performance of the distributed control system was evaluated by comparison of uncontrolled and controlled system responses, which were in the frequency range of 0-250 Hz, the first six natural frequencies of the beam. The reduction of vibration responses of the system is shown in Figure 2-4.

## Conclusions

In this paper decentralized vibration control of a simply supported beam has been implemented using networked embedded systems. It is shown that the reduction of system vibration is realized with a decentralized vibration control method. The approach

used in this research can be extended to active noise control of other structures with networked embedded systems.

## Acknowledgements

This research was supported by the DARPA Information Exploitation Offices' Network Embedded System Technology (NEST) program and a National Science Foundation CAREER Award No. CMS-0134224.

## References

[1] C. J. Swigert and R. L. Forward, "Electronic Damping of Orthogonal Bending Modes in a Cylindrical Mast - Theory," Journal of Spacecraft and Rockets, Vol. 18, No. 1, 1981, pp. 5-10.

[2] T. Bailey and J. E. Hubbard, Jr., "Distributed Piezoelectric Polymer Active Vibration Control of a Cantilever Beam," Journal of Guidance, Control, and Dynamics, Vol. 8, No. 5, 1985, pp. 605-611.

[3] Y. St-Amant and L. Cheng, "Simulations and experiments on active vibration control of a plate with integrated piezoceramics," Thin-Walled Structures, Vol. 38, No. 2, 2000, pp. 105-123.

[4] S.-B. Choi, "Alleviation of chattering in flexible beam control via piezofilm actuator and sensor," AIAA Journal, Vol. 33, No. 3, 1995, pp. 564-567.

[5] K. D. Frampton, "Decentralized Control of Structural Acoustic Radiation," Proceedings of IMECE 2001, New York, 2001.

[6] M. Strassberger and H. Waller, "Active noise reduction by structural control using piezo-electric actuators," Mechatronics, Vol. 10, No. 8, 2000, pp. 851-868.

[7] N. W. Hagood, W. H. Chung, and A. von Flotow, "Modelling of piezoelectric actuator dynamics for active structural control," 31st AIAA/ASME/ASCE/AHS/ASC Structures, Structural Dynamics and Materials Conference, Long Beach, CA, USA, 1990.

[8] R. Clark, W. Saunders, and G. Gibbs, *Adaptive Structures: Dynamics and Controls*, John Wiley & Sons, New York, 1998.

[9] E. Scholte and R. D'Andrea, "Active Vibro-acoustic Control of a Flexible Beam Using Distributed Control," 2003 American Control Conference, Jun 4-6 2003, Denver, CO, United States, 2003.

[10] M. J. Balas, "Direct Velocity Feedback Control of Large Space Structures," Journal of Guidance Control and Dynamics, Vol. 2, No. 3, 1979, pp. 252-253.

[11] W. Levine and M. Athans, "On the determination of the optimal constant output feedback gains for linear multivariable systems," IEEE Transactions on Automatic Control, Vol. 15, No. 1, 1970, pp. 44-48.

[12] J. Elson, L. Girod, and D. Estrin, "Fine-Grained Network Time Synchronization using Reference Broadcasts," the Fifth Symposium on Operating Systems Design and Implementation, Boston, MA, 2002.

# CHAPTER III

## MANUSCRIPT 2

## EXPERIMENTS ON DISTRIBUTED ACTIVE VIBRATION CONTROL OF A SIMPLY SUPPORTED BEAM

Tao Tao and Kenneth D Frampton

Vanderbilt University

Nashville, TN 37235, USA

(Submitted to Smart Materials and Structures)

### Abstract

In this paper the application of distributed vibration control for a flexible structure is studied both analytically and experimentally. The purpose is to investigate the effectiveness of distributed vibration control strategies and compare them with centralized and decentralized methods. A simply supported beam is chosen as the illustrative flexible structure. A distributed control architecture is designed based on a system identification model and is used to minimize vibration due to broadband disturbances. Experimental results are presented for the control of the beam's vibration modes under 600 Hz. It is shown that the distributed control architecture presented here approaches the performance of a traditional centralized controller employing the same control effort. In addition, in comparison to centralized control, the distributed controller

has the advantages of scalability for application in large systems and that it will continue to perform even when some processors fail, although probably with diminished capability.

## Introduction

Active vibration control is a popular strategy used to reduce vibration and noise radiation from flexible structures[1,2,3,4]. For large-scale systems such as space structures, active vibration control has the advantage of reduced weight over passive damping methods[5]. One of the earliest works in the field of active vibration and acoustic control was published by Fuller[3]. Feed-forward control was used to reduce narrow band acoustic radiation with structural actuators, and considerable noise attenuations were achieved with this approach[6,7]. Others used feedback control to reduce stochastic disturbances such as turbulent boundary layer noise[8,9,10] However, most active vibration control designs rest on the presupposition of centrality: one controller processes all sensor data to generate actuator inputs in order to reduce the structural vibrations. Such centralized control designs have been used in many practical situations. However, when large-scale systems are considered, numerous sensors and actuators are required resulting in an overwhelming computational burden on the centralized controller.

Recent advances in Micro-Electro-Mechanical systems (MEMS) and embedded system technologies[11] has enabled the use of decentralized and distributed systems for the control of large-scale systems. Such system offer great promises in overcoming the scalability issues associated with centralized control. A decentralized control system consists of more than one subsystem, each operating independently, to achieve overall system vibration reduction[2,12]. Decentralized control was also applied to active structural

vibration and acoustic control recently[13,14,15,16]. In comparison to centralized control, decentralized control is more scalable, however, since each controller is designed based only on local sensor information (rather than all available sensor data), the performance is usually not as good as with a centralized control system.

One possible way of overcoming scalability issues while achieving performance similar to that of centralized control is to use distributed control. A distributed control system consists of numerous localized controllers called nodes. Each node has a controller; sensors and actuators; and a means of communicating with other nodes in the system. The field of distributed control has been studied for over 30 years[17]. Most of this work was concerned with "weakly connected" systems, in which nodes are weakly coupled to each other and each node only experiences a few of the degrees of freedom of the entire system[18,19]. Distributed control has been studied for reduction of noise radiation of flexible structures[20] and for vibrating structures[21]. Control systems based on such a platform would be able to share sensor information in order to work cooperatively to achieve improved performance. Furthermore, a distributed control system can reduce the computation burden on each subsystem, and limit the sensor information that is exchanged, so that the overall system is scalable for use in large-scale systems[20,21].

The primary contribution of this work is to investigate the use of distributed control for active structural vibration control. A decentralized architecture can be extended to a distributed system by employing some degree of inter-node cooperation, and thus the advantage of the decentralized architecture can be retained while achieving performance approaching that of centralized control. The work presented here begins with a description of the experimental platform. This is followed by a discussion of

system identification and comparisons with theoretical models. Next, the distributed control design, based on H2 control techniques, is explained. Finally, the performance of the distributed control method is evaluated and compared to centralized and decentralized control systems.

## Experimental Setup

In order to validate the distributed controller design proposed here, a simply supported beam experiment was constructed as shown in Figure 3-1. The beam is clamped at the both ends, with grooves machined near both ends to approximate simply supported boundary conditions. This work focuses on the vibrations from 0-600Hz which includes the first nine modes. These nine natural frequencies have been theoretically predicted to be: 6.5, 26.1, 58.7, 104.3, 163.0, 234.7, 319.5, 417.3, and 528.2 Hz. System identification results discussed later show that the actual natural frequencies match the theoretical values very well.

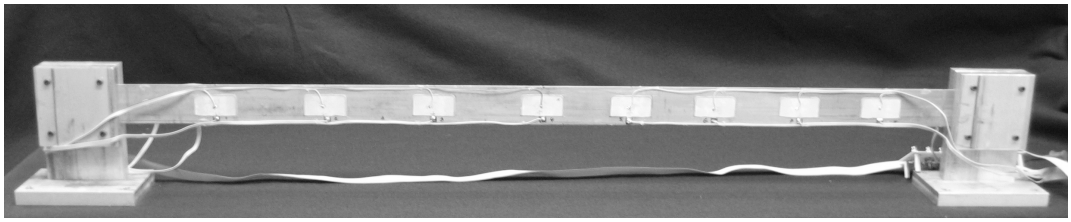

**Figure 3-1**. The experimental beam with multiple sensor/actuator pairs.

Lead Zirconate Titanate (PZT) patches were used as sensors and actuators. Since PZT materials have direct and inverse piezoelectric effect when an external load is

applied, an electric charge is produced at the surface of the material. Similarly, when a voltage is applied to the material, a strain is induced within[4]. Sensor and actuator patches were attached on opposite sides of the beam, and at the same locations. A band-limited voltage was applied to PZT1 in Figure 3-1 (left most transducer) as the disturbance, whose coordinate along the beam is 0.11m. Four collocated pairs of PZT patches, PZT2, PZT3, PZT6 and PZT8 in Figure 3-1, were used as control transducers, and their coordinates are 0.25m, 0.39m, 0.75m and 0.98m respectively. The size of each PZT patch is 0.055m by 0.027m.

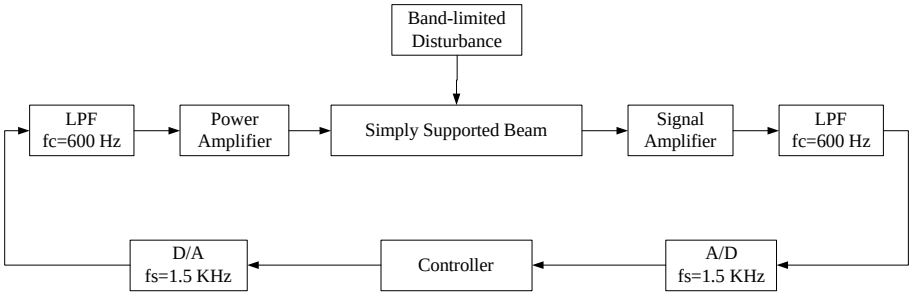


**Figure 3-2**. Block diagram of closed-loop system.

The instrumentation arrangement is shown schematically in Figure 3-2. Band-limited white noise (0-600 Hz) was used as the disturbance to excite the beam, and the beam vibration was measured with PZT patches. The sensor signals were amplified and filtered with 4-pole Butterworth low-pass filters having a cut-off frequency of 600 Hz. The distributed controller was implemented on a dSPACE DS1103 PPC board with AD/DA conversions. The control output was amplified by a 790A06 power amplifier from PZB Piezotronics, Inc.

**System Identification**

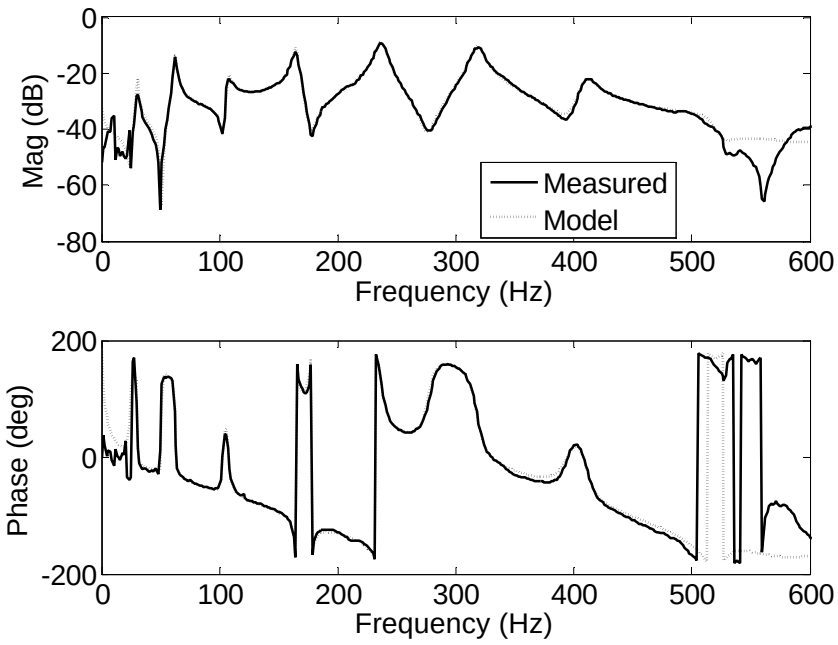


**Figure 3-3**. Experimental and analytical frequency responses from the disturbance to sensor 1.

In order to obtain the most accurate system model from which controllers were designed a system identification approach was used. When the vibration displacements of the beam are small, a linear model can reasonably represent the system. Four sensors and four actuators were used for the control system resulting in sixteen transfer functions from the inputs to outputs. In addition, the path between disturbance and sensors was also identified. Band-limited white noise was applied to each actuator and sensor data was collected from each sensor. This data was used to get the Auto-Regression with extra inputs model (ARX), shown in equation (1).

$$y(t) + a_1 y(t-1) + \ldots + a_n y(t-n) = b_1 u(t-1) + \ldots + b_m u(t-m) \quad (1)$$

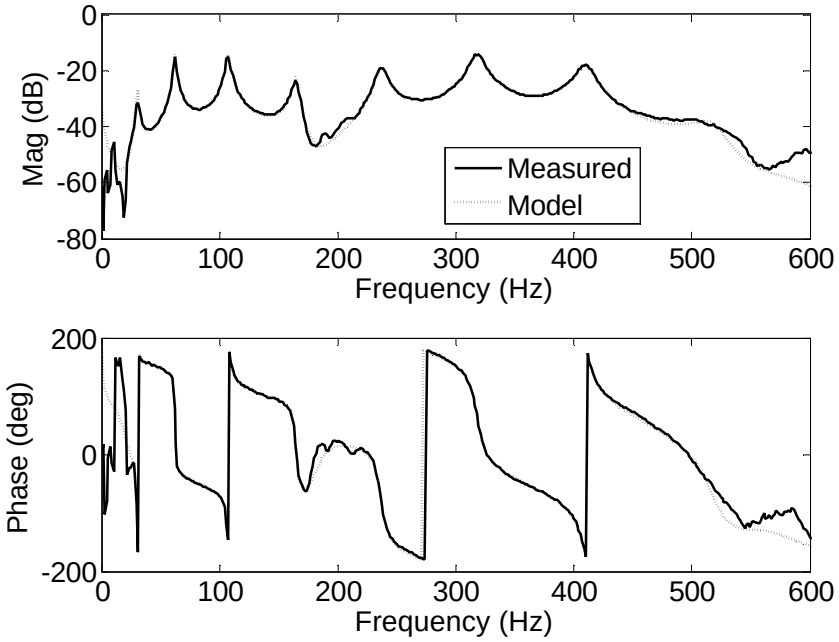


**Figure 3-4**. Experimental and analytical frequency responses from the disturbance to sensor 4.

A batch least squares solution was used to find the desired ARX parameters, and a multi-input multi-output (MIMO) state space model was then derived from the ARX model[22]. In order to choose an appropriate system order and obtain the optimal system model, the frequency responses of all signal paths were measured and system identification was performed. The final order of the identified model was chosen to be 36, since it provided the best fit with the lowest order. In Figures 3-3 and 3-4, the transfer functions measured directly from system identification data are depicted with solid lines, and the transfer functions derived from the corresponding state-space model were shown with dotted lines. As shown, the state space model represents the beam dynamics very well, in both magnitude and phase of the system response. The discrepancy at the low frequency range (0-20 Hz) is due to the effect of environmental noise on the response

measurements. All other system transfer functions compared similarly well. Furthermore, the frequency peaks of the identified model occur at 8.7, 29.3, 61.0, 105.9, 165.4, 235.8, 318.9, 413.3, and 515.4 Hz. These values compare very well with the theoretical values discussed earlier.

## Distributed Controller Design

The distributed controller design in this section is based on centralized $H_2$-optimal control theory which has been proven effective at attenuating structural vibration. The centralized $H_2$-optimal controller is extended here to control vibrations under a distributed architecture. The basic block diagram of $H_2$ closed-loop system is shown in Figure 3-5, where G is the generalized plant, K is the controller, w is the exogenous input vector consisting of the disturbance and sensor noises; u is the control signal vector; z is the output vector to be minimized, which consists of filtered actuator signals, system states and plant outputs; and y is the plant output vector. The system from w to z is denoted with the transfer function $T_{zw}(s)$, and the goal of $H_2$-optimal control is to compute an internally stabilizing controller, K, which minimizes $\|Tzw\|_2$ . Details concerning the calculation of the optimal controller K can be found in Reference[23]. Suitable optimization weights were chosen in order to ensure that all closed loop systems had the same $H_2$-norm between the disturbance and all control inputs. This resulted in equal global control effort among all systems.

Three types of controllers were designed for these experiments. These included a centralized controller, a set of decentralized controllers, and a set of distributed controllers. The centralized controller was designed using all 4 sensors and actuators. The

decentralized architecture consisted of four locally optimal SISO compensators. Each compensator operated independently using its own sensor and actuator in order to achieve the global control performance.

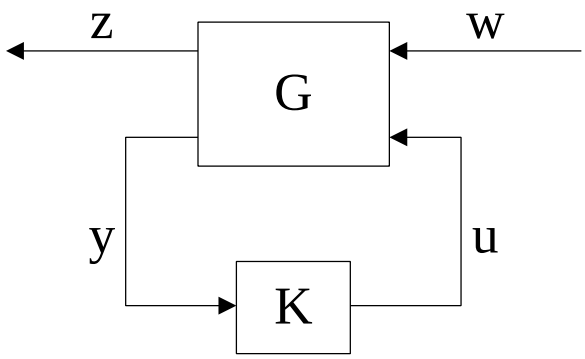


**Figure 3-5.** Basic $H_2$ closed-loop system.

In the distributed control architecture each node shared instantaneous sensor signals with the nodes on either side. In this manner each nodes local compensator used its own sensor signal, as well as those communicated from the two neighboring nodes, to construct the local actuator signal. Thus, two of the local compensators are three-input single-output control system. However, the leftmost and rightmost compensators were two-input single-output. Such an architecture could easily be extended to larger scale systems as has been demonstrated analytically[8].

The distributed controller is designed based on $H_2$ optimal control technique, in the same way as the centralized controller design. Each distributed compensator is a MISO system in the following generic form:

$$U_i = -\mathbf{K}(s)Y_{i-1,i,i+1} \tag{2}$$

where ui is the local control signal, K(s) is the optimal H2 controller and yi-1, i, i+1 is the sensor vector available for the local control design. As in the centralized controller design, the sensor penalty was adjusted so that all control architectures have the same global control effort in order to ensure a fair comparison.

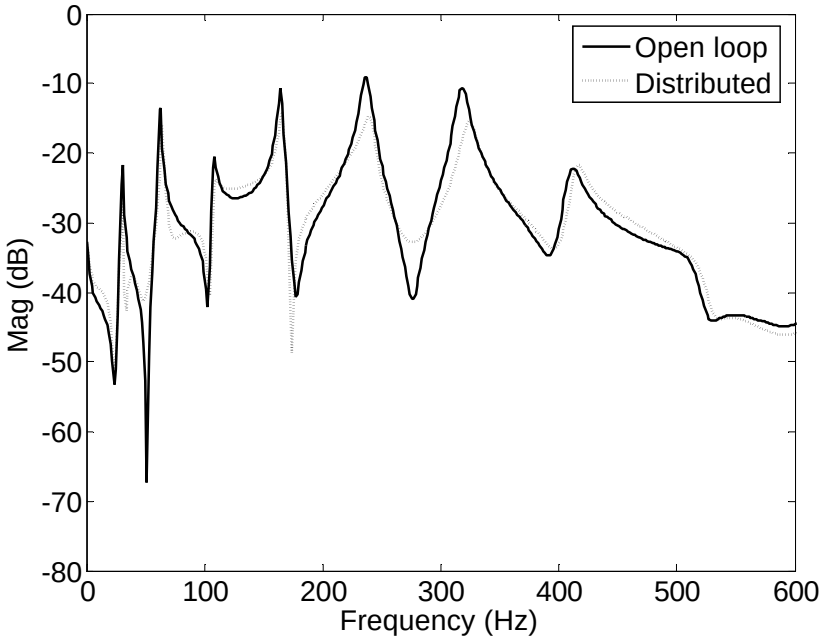


**Figure 3-6**. Transfer function from the disturbance to sensor 1 in simulation.

The theoretical distributed control performance is demonstrated in Figure 3-6 which shows the transfer function from disturbance to sensor 1. The data in Figure 3-6 were created by designing a set of distributed compensators and closing the loop on the system identification model. As is shown, the vibration amplitude at 235 Hz was reduced by about 6 dB. The H2 norm of closed-loop system in Figure 3-6 was 0.09, while the H2 norm of the open-loop system was 0.12, demonstrating that the distributed controller is capable of reducing the overall beam vibration levels.

## Experimental Results

Each of the three described control architectures was implemented on the experimental platform discussed previously. The control performance of the distributed controller was compared with that of the centralized and decentralized controllers. The control performance is represented by the transfer function from the disturbance to the first sensor, as shown in Figure 3-7. Transfer functions from the disturbance to other sensors showed similar results.

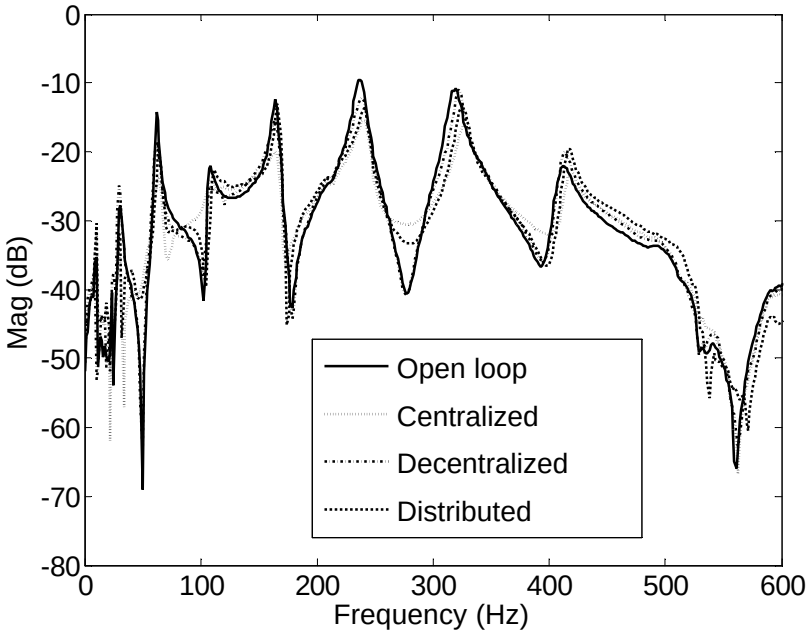


**Figure 3-7.** Experimental frequency response from the disturbance to sensor 1.

In order to fairly compare the performance of these three controllers, the global control efforts were tuned to be equal. As discussed previously, each compensator design was checked to ensure equal control effort based on simulations using the identified model. Furthermore, the control effort was checked experimentally by computing the total control signal power in each case (for equal disturbance power). When experimental

discrepancies in control effort were found the compensator was redesigned and the control effort was checked again.

As shown in Figure 3-7, the centralized controller has the best performance, the decentralized controller has the worst performance, and the performance of the distributed controller falls in between. This comparison holds for all of the modal peaks as well as the total vibration power reductions shown in Table 3-1. These results compare well with previous analytical distributed control results[21], decentralized results[16], and centralized results[4].

**Table 3-1**. Various overall vibration reduction with different architectures.

| Control Architecture | Overall Reduction of Vibration |
|---|---|
| Centralized | 7.51 |
| Decentralized | 3.30 |
| Distributed | 4.17 |

In comparison to the decentralized controller whose control signals are based only on local sensors, the distributed controller takes advantage of more sensor data including the local sensor, and a better overall control performance is demonstrated. Compared with the centralized controller, there is less computation when each actuator force is calculated since not all sensor data are needed for each actuator.

## Conclusions

In this paper distributed vibration of a simply supported beam has been implemented, and it is shown that the distributed controller has a better control performance than local control. The distributed controller also reduces the computation

required relative to a centralized controller, which is desirable for embedded control systems. The approach used in this work can be extended to active noise control and to applications in large-scale systems.

## Acknowledgements

This work was supported by the DARPA Information Exploitation Offices' Network Embedded System Technology (NEST) program and a national Science Foundation CAREER Award No. CMS-0134224.

## References

[1] R. L. Clark and C. R. Fuller, "Experiments on active control of structurally radiated sound using multiple piezoceramic actuators," Journal of the Acoustical Society of America, Vol. 91, No. 6, 1992, pp. 3313-3320.

[2] S. J. Elliott, P. Gardonio, T. C. Sors, and M. J. Brennan, "Active vibroacoustic control with multiple local feedback loops," Journal of the Acoustical Society of America, Vol. 111, No. 2, 2002, pp. 908-915.

[3] C. R. Fuller, "Experiments on reduction of aircraft interior noise using active control of fuselage vibration," Journal of the Acoustical Society of America, Vol. 78, No. S1, 1985, pp. S88.

[4] R. L. Clark, W. R. Saunders, and G. P. Gibbs, *Adaptive Structures: Dynamics and Control*, Wiley, New York, 1998.

[5] S. M. Kuo and D. R. Morgan, "Active noise control: a tutorial review," Proceedings of the IEEE, Vol. 87, No. 6, 1999, pp. 943-975.

[6] R. L. Clark and D. E. Cox, "Multi-variable structural acoustic control with static compensation," Journal of the Acoustical Society of America, Vol. 102, No. 5, 1997, pp. 2747-2756.

[7] R. L. Clark and C. R. Fuller, "Active structural acoustic control with adaptive structures and wavenumber considerations," Journal of Intelligent Material Systems and Structures, Vol. 3, No. 2, 1992, pp. 296-315.

[8] W. T. Baumann, "An adaptive feedback approach to structural vibration suppression," Journal of Sound and Vibration, Vol. 205, No. 1, 1997, pp. 121-133.

[9] K. W. Eure, "Adaptive predictive feedback techniques for vibration control," in *Electrical Engineering*. Blacksburg, VA: Virginia Polytechnic Institute and State University, 1998.

[10] L. Hakansson, I. Claesson, and P. O. H. Sturesson, "Adaptive feedback control of machine-tool vibration based on the filtered-x LMS-algorithm," Journal of Low Frequency Noise Vibration and Active Control, Vol. 17, No. 4, 1998, pp. 199-213.

[11] I. D. McCammon and S. C. Jacobsen, "Communication and control for distributed microsystems," IEEE Control Systems Magazine, Vol. 10, No. 2, 1990, pp. 48-50.

[12] K. D. Frampton, "Decentralized control of structural acoustic radiation," Proceedings of IMECE 2000, New York, NY, 2001.

[13] O. N. Baumann, W. P. Engels, and S. J. Elliott, "A comparison of centralized and decentralized control for the reduction of kinetic energy and radiated sound power," Proceedings of Active04, Williamsburg, VA, 2004.

[14] P. Gardonio, E. Bianchi, and S. J. Elliott, "Smart panel with multiple decentralized units for the control of sound transmission. Part I: theoretical predictions," Journal of Sound and Vibration, Vol. 274, No. 1-2, 2004, pp. 163-192.

[15] P. Gardonio, E. Bianchi, and S. J. Elliott, "Smart panel with multiple decentralized units for the control of sound transmission. Part II: design of the decentralized control units," Journal of Sound and Vibration, Vol. 274, No. 1-2, 2004, pp. 193-213.

[16] E. Bianchi, P. Gardonio, and S. J. Elliott, "Smart panel with multiple decentralized units for the control of sound transmission. Part III: control system implementation," Journal of Sound and Vibration, Vol. 274, No. 1-2, 2004, pp. 215-232.

[17] N. Sandell, Jr., P. Varaiya, M. Athans, and M. Safonov, "Survey of decentralized control methods for large scale systems," IEEE Transactions on Automatic Control, Vol. 23, No. 2, 1978, pp. 108-128.

[18] D. J. Stilwell and B. E. Bishop, "Platoons of underwater vehicles: communication, feedback and decentralized control," IEEE Control Systems Magazine, Vol. 20, No. 6, 2000, pp. 45-52.

[19] M. J. B. Krieger, J. B. Billeter, and L. Keller, "Ant-like task allocation and recruitment in cooperative robots," Nature, Vol. 406, No. 6799, 2000, pp. 992-995.

[20] E. Scholte and R. D'Andrea, "Active vibro-acoustic control of a flexible beam using distributed control," American Control Conference, Denver, CO, 2003.

[21] K. D. Frampton, "Distributed group-based vibration control with a networked embedded system," Smart Materials & Structures, Vol. 14, No. 2, 2005, pp. 307-314.

[22] L. Ljung, *System Identification: Theory for the User*, Prentice Hall, Upper Saddle River, NJ, 1998.

[23] K. Zhou, J. C. Doyle, and K. Glover, *Robust and Optimal Control*, Prentice-Hall, Upper Saddle River, NJ, 1995.

# CHAPTER IV

# MANUSCRIPT 3

## EXPERIMENTAL COMPARISON OF SENSOR GROUPING FOR DISTRIBUTED VIBRATION CONTRL

Tao Tao and Kenneth D. Frampton

Vanderbilt University

Nashville, TN 37235, USA

(Submitted to Journal of Sound and Vibration)

### Abstract

In this paper the performance of a distributed vibration control system based on various sensor grouping schemes is demonstrated. The benefit of using sensor groups is that the result control architecture is scalable for use in large-scale systems. A simply supported beam is chosen as the illustrative flexible structure, and two types of sensor grouping strategies are considered: groups based on physical proximity and groups based on modal sensitivity. The global control objective is to minimize the beam's vibrational response under 600 Hz with a performance that approaches that of traditional centralized control. Experimentally obtained control performance results are compared and discussed which demonstrate the effectiveness of the two distributed grouping

approaches. It is also shown that these distributed control methods approach the performance of traditional centralized control as the group size is increased.

## Introduction

Although active control has been used to reduce structural vibrations for many years[1,2,3,4], the application of active vibration control on large-scale systems has achieved little success due to the scalability limitations of traditional centralized control architectures. In centralized control, one controller processes all sensor data to generate optimal actuator inputs in order to reduce the structural vibrations. Centralized control strategies, such as adaptive feedback and adaptive feed-forward, are chosen for different vibration applications[3,5]. Thus, there is an overwhelming, even impractical, computational burden on the centralized controller, when large-scale systems are considered. Recent advances in Micro-Electro-Mechanical systems (MEMS) and embedded system technologies have enabled the applications of distributed control designs[6], which is more scalable compared with centralized control and suitable for large-scale systems.

A distributed control system normally consists of numerous localized controllers called nodes. Each localized controller has a sensor, an actuator and a means of communicating with other controllers in the system[7,8,9,10,11]. The goal of distributed control systems is to achieve a global performance by sharing sensor information among the localized controllers. This is in contrast to decentralized control whose localized controllers work independently to achieve a global performance[12,13,14,15,16]. Distributed control has been studied for over 30 years, but most of these studies were concerned with

"weakly connected" systems, where each local controller only experiences a few of the degrees of freedom of the entire system (e.g. robotic swarms). Recently, distributed control has been studied for noise radiation reduction and vibration reduction[9,17,18,19] which requires control design approaches suitable for strongly connected systems. While these efforts have demonstrated the suitability and scalability of distributed architectures, their performance has not been demonstrated experimentally.

One of the most important, enabling technologies for distributed control systems is distributed middleware. Middleware is software that operates between the operating system and the application (the control law in this case)[20,21]. There are numerous middleware services that would be important to the deployment of a distributed control system. These include network discovery; clock synchronization; distributed resource allocation; network communications routing; and many others. The service that would most affect the performance of distributed control is group management and the inter-node communications that it provides[22,23,24]. Group management services manage the formation and organization of groups of nodes; provide for the communication among nodes; maintain routing tables; execute leader election and group consensus applications; clock synchronization; and many other tasks. The reason that group management services are important to distributed control is that they offer the means by which scalable distributed control architectures can be constructed.

Scalability in a distributed control system is very important to its success. This is because as a distributed control system becomes larger the number of nodes increases, resulting in an exponential increase in network communication traffic. However, the ability of the network to transmit this information does not scale up as quickly as the

volume of information. Therefore, in order to be scalable the amount of information transmitted must be limited. This can be achieved by forming nodes into groups, and limiting inter-node communications to within those groups. Therefore, by designing control laws that depend only on sensor information from within the group (instead of from all sensors), the network traffic can be limited and the scalability of the system can be ensured. Since these group management services provide scalable communications they provide a promising framework for the current work: that is to develop distributed control algorithms which utilize groups of sensors. While some investigations have been undertaken to include specific models of middleware[25,26] the middleware itself is not included in the simulations presented here. Rather, their existence has served as the framework for designing control systems that take advantage of their capabilities.

The purpose of this work is to experimentally demonstrate distributed control on a non-weakly connected system and to compare sensor grouping techniques that will result in scalable distributed control architectures[9,27]. A simply supported beam with six pairs of piezoelectric transducers acting as sensors and actuators is the active structure investigated. The work presented here begins with a description of the experimental platform, followed by system identification results. Then, distributed controllers are designed based on a system identification model and $H_2$ optimal control[9,27,28]. Finally, the performance of different control strategies is demonstrated and compared, including centralized control, decentralized control, distributed control based on modal grouping, and distributed control based on physical proximity. For the distributed control based on physical proximity, groups of varying size are also compared.

## Experimental Setup

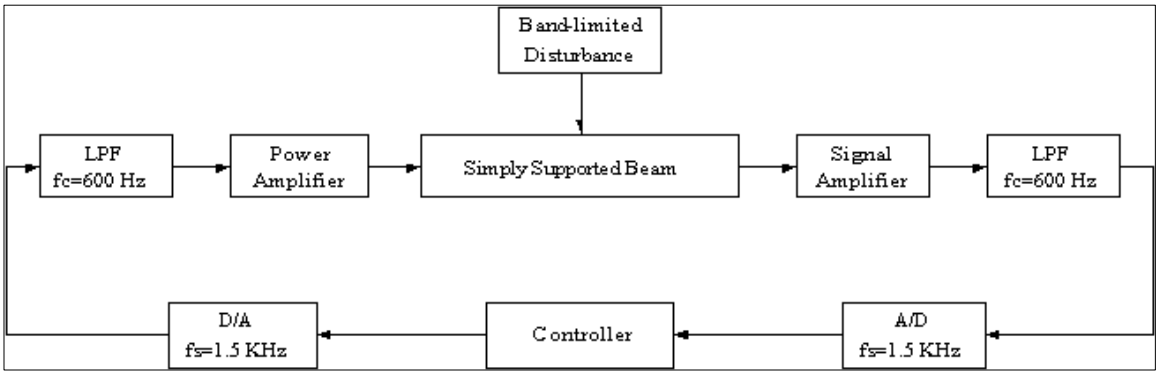


**Figure 4-1**. Block diagram of the experimental setup

The instrumentation arrangement used in the experimental setup is shown schematically in Figure 4-1. The simply supported beam is disturbed by band-limited white noise (0 - 600Hz) , and sensor signals are amplified and filtered with four-pole Butterworth low-pass filters. Distributed controllers are implemented on a dSPACE DS1103 PPC board, and control signals are amplified by a 790A06 power amplifier from PZB Piezotronics, Inc.

**Table 4-1**. Physical parameters of the experimental beam.

| Physical parameters | Values |
|---|---|
| Density | 2700 (kg/m3) |
| Thickness | 0.0032 (m) |
| Length | 1.0650 (m) |
| Width | 0.0508 (m) |
| Young's Modulus | 73.1E9 (Pa) |

The physical system is a beam made of aluminum 2024-T4 with physical parameters as listed in Table 4-1. The beam is clamped at both ends, with grooves machined near both ends to approximate the simply supported boundary condition[29]. System identification results have shown that the beam's dynamic response is very close to theoretical predictions for a simply supported beam.

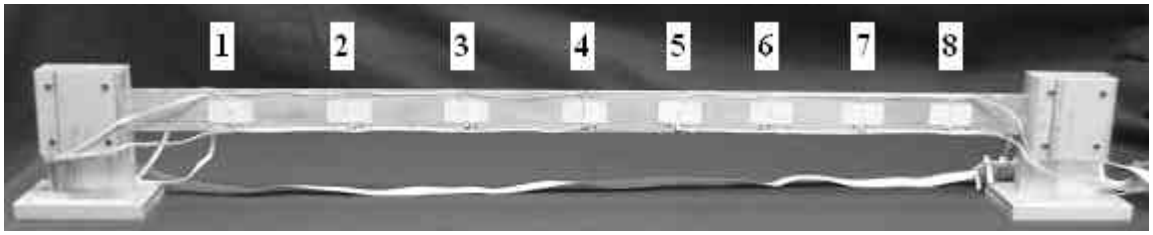


**Figure 4-2**. The experimental beam with multiple sensor/actuator pairs.

Lead Zirconate Titanate (PZT) transducers are attached along the beam acting as sensors and actuators, as shown in Figure 4-2. The size of each PZT patch is 0.055m by 0.027m. PZT patches are not evenly distributed along the beam, and the coordinates from left end of the beam to centers of patches are: 0.11m, 0.25m, 0.38m, 0.53m, 0.64m, 0.76m, 0.87m, and 0.98m. All sensors are on the same side of the beam, and all actuators are on the opposite side. The band-limited noise is applied to PZT1 as the disturbance. It is known that the transducer placements will affect control performance, and so the transducers were chosen to maximize sensitivity to the structural modes below 600 Hz. . The six collocated pairs of transducers selected were: PZT2, PZT3, PZT4, PZT6, PZT7 and PZT8 along the beam (as shown in Figure 4-2).

## System Identification

As specified previously, the system model obtained from theoretical derivation matches the experimental result well. However, since the control performance depends on the accuracy of the system model, the dynamics of the beam were obtained using experimental system identification. Six sensors and six actuators were used for the control system, resulting in 36 transfer functions from the inputs to outputs. In addition, the path between disturbance and all sensors was also identified. A band-limited white noise input was applied to each actuator, and then all sensor and actuator data were collected to derive the Auto-Regression with eXtra inputs (ARX) model:

$$y(t) + a_1 y(t-1) + \ldots + a_n y(t-n) = b_1 u(t-1) + \ldots + b_m u(t-m) \tag{1}$$

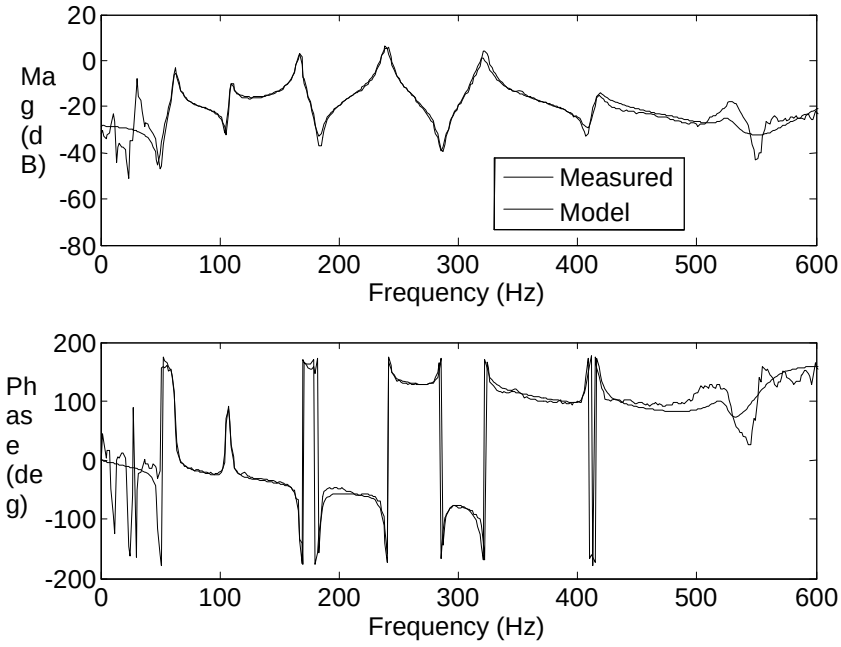


**Figure 4-3**. Experimental and analytical frequency responses from the disturbance to sensor 1.

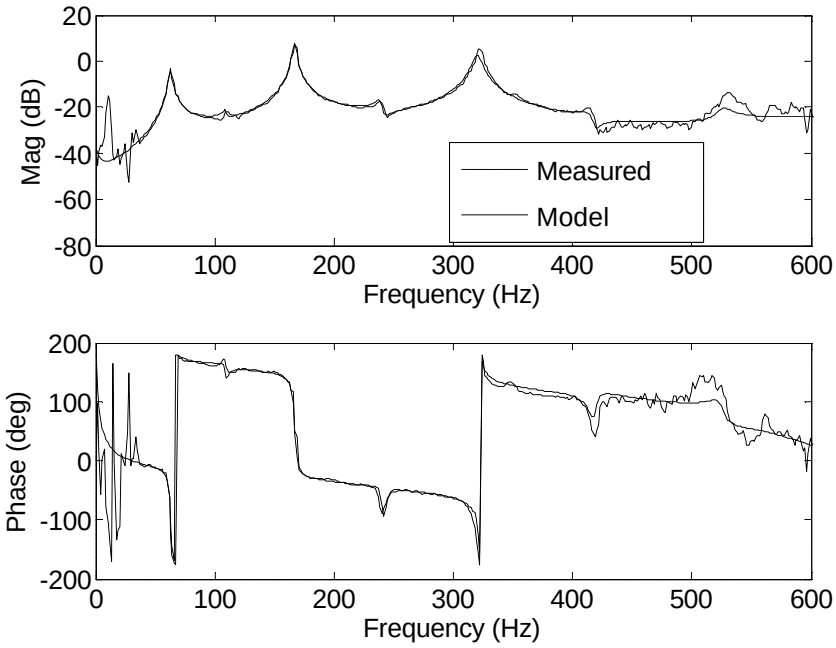


**Figure 4-4**. Experimental and analytical frequency responses from the disturbance to sensor 3.

The ARX parameters were obtained using a batch least squares solution, and then a multi-input multi-output (MIMO) state-space model was derived from the corresponding ARX model.

After exploring various model sizes a 36 state model was selected for control design use. Experimental and analytical frequency responses of two signal paths are shown in Figures 4-3 and 4-4. In Figure 4-3, the solid lines represent the transfer function from the disturbance to sensor 1 estimated directly from system identification data, while the dotted lines represent the transfer function of the a state-space system identification model with 36 states. It is clearly shown that the state-space model represent the beam dynamics very well, in both magnitude and phase. Similarly, the transfer function from the disturbance to sensor 3, shown in Figure 4-4, demonstrates a

good match between experimental and analytical data. All other signal paths have similar results.

Another important characteristic of the control system is also shown in Figures 4-3 and 4-4, which is the unique modal sensitivity for different sensors. Note in Figure 4-3 that sensor 1 is most sensitive to vibrational modes at 165.4Hz, 235.8Hz and 318.9Hz, while sensor 3 is most sensitive to vibrational modes at 61.0Hz, 165.4Hz and 318.9Hz as shown in Figure 4-4. These modal sensitivities will serve as the criteria by which groups are formed when implementing modal the grouping strategy discussed later.

## Distributed Controller Design

### $H_2$ Optimal Design

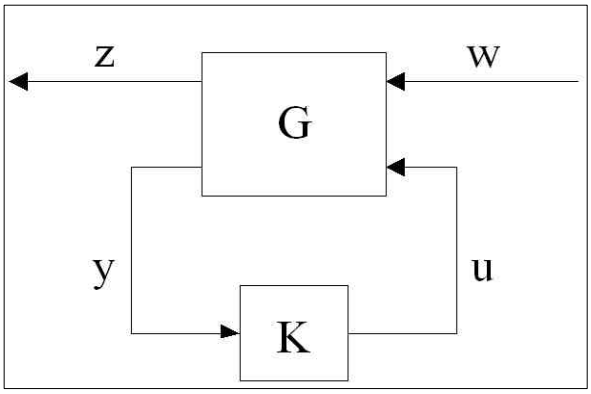


**Figure 4-5**. Basic H2 closed-loop system.

All controllers in this work are designed based on traditional $H_2$ optimal control theory[28,30]. Such $H_2$ optimal control has been proven effective and robust at attenuating structural vibration in centralized strategy, and it is extended here to a distributed architecture. Existing distributed control design approaches are not applicable to

structural vibration systems due to the strongly connected nature of their dynamics. However the arrangement and implementation in a distributed manner is unique.

The basic block diagram of $H_2$ closed-loop system is shown in Figure 4-5, where **G** is the generalized plant, **K** is desired controller, **w** is the exogenous input vector consisting of disturbance and sensor noise, **u** is the control signal vector, and **y** is the plant output vector. In Figure 4-5, **z** is the output to be minimized which consists of the filtered actuator signals system states and plant outputs. The states are weighted so that those states associated with the modes targeted for attenuation (163 Hz, 234 Hz and 320 Hz) are penalized more than the other states. Including all states helps to prevent energy spillover in to untargeted modes. The goal of $H_2$ optimal control is to compute an internally stabilizing controller **K**, which minimizes the transfer function from the disturbance to the performance, $\|Tzw\|_2$. After each distributed controller has been designed, all compensators were connected to the plant in parallel, as would occur in a network-based implementation of distributed control. Details concerning the calculation of the optimal controller **K** can be found in references[28,30].

**Geographic Grouping Distributed Control**

As described previously, in order to create a distributed control system each localized controller shares sensor information within a group of other controllers in the distributed control architecture. Then, each localized controller is designed according to the sensor data that is available to it using the $H_2$ control design described previously. Therefore, each local controller is locally optimal, but the global system is not optimal. In order for such an architecture to be scalable (i.e. able to be functional in systems with

numerous sensors) the groups must contain only a fraction of the total sensors in the system. One way to achieve this is to organize the sensors based on close physical proximity. Such groups are referred to here as geographic groups and the group size is defined by a groups "reach." The reach of a localized controller is defined as the number of sensors to a particular controllers right and left (plus its own sensor) that are available to it for control implementation. For example, in a distributed control system of reach 1, each local compensator is designed based on its own sensor signal, the signal from the sensor to its left, and the signal from the sensor to its right. Thus, the local subsystems are three-input single-output control system with the exception of the leftmost and rightmost compensators, which are two-input single-output systems.

Actual implementation of such a distributed control system would require the ability to create and manage such groups. This would be accomplished through distributed middleware. When the sensor network is started up a protocol is begun which, among other things, involves localized processors discovering what other processors are present in the control network. Then, the group management middleware would begin to form groups based on pre-defined rules and create message routing tables to allow for sensor data communication. Such network communications software are not part of the experiments presented here, the specific communications interconnections are included. These communications connections consist of connecting each distributed controller to the other controllers to organize them into groups. The result is a system feedback connection that exactly matches the global system connection that would result if actual group management middleware were employed. However, this method of simulating network communications is equivalent to assuming that network communications occur

instantaneously or fast enough to meet real-time discrete sampling requirements. In other words, it is assumed that the network is capable of communicating sensor information at a rate that is much faster than the system bandwidth. Previous work has investigated the inclusion of middleware simulations and the resulting network communications delay on feedback performance[26].

As mentioned previously, each of the local compensators are designed based on H2 optimal control technique. To ensure fair comparisons among different control architectures, control penalty weights were chosen so that all closed-loop systems had the same H2 norm between the disturbance and all control input signals.

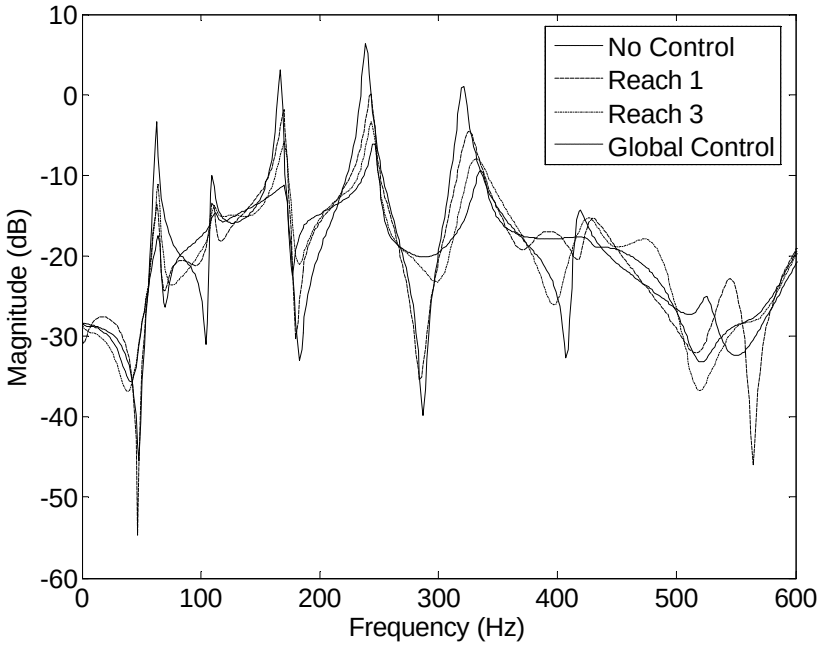


**Figure 4-6**. Transfer function from the disturbance to sensor 1 in simulation.

In Figure 4-6, four system frequency responses are compared including: the open loop system; distributed control with reach of 1; distributed control with reach of 3; and a

centralized controller. These results are based on simulations for the experimental system described previously. Control performances are demonstrated with transfer functions from the disturbance to sensor 1, while other system transfer functions showed similar vibration reduction results. The simulation results show that, as one might expect, the performance improves as the reach is increased and approach the performance of centralized global control which has the best vibration reduction.

**Modal Grouping Distributed Control**

**Table 4-2**. Modal sensitivity to three dominant vibrational modes.

| | 163Hz ($5^{th}$) | 234Hz ($6^{th}$) | 320Hz ($7^{th}$) |
|---|---|---|---|
| Sensor 1 | 1.5 | 1.9 | 1.6 |
| Sensor 2 | 1.1 | 1.1 | 1.5 |
| Sensor 3 | 2.3 | 0.1 | 1.8 |
| Sensor 4 | 2.2 | 1.2 | 0.1 |
| Sensor 5 | 0.6 | 0.4 | 1 |
| Sensor 6 | 1.9 | 1.6 | 1.5 |

In distributed control system based on modal grouping strategy, a group contain a fixed number of localized controllers that posses the highest sensitivity to the vibrational mode to be targeted by that group. Three dominant vibrational modes are targeted for attenuation: 163 Hz, 234 Hz and 320 Hz. Therefore, three groups are formed each containing 3 sensors. The sensitivity of each sensor to each mode is determined by the frequency response magnitude of that specific signal path.

**Table 4-3**. Transducer membership in groups based on modal sensitivity

| Mode | Sensors in the 3-member group |
|---|---|
| 163Hz ($5^{th}$) | 3, 4, 6 |
| 234Hz ($6^{th}$) | 1, 4, 6 |
| 320Hz ($7^{th}$) | 2, 3, 5 |

The sensitivities of each sensor are shown in Table 4-2 and the grouping is shown in Table 4-3. In the group targeting the $7^{th}$ vibrational mode sensor 5 is included even though it is not among the top three transducers sensitive to the mode, so that all transducers in the whole system will be used in the distributed system.

As for the geographic grouping, each controller is designed as a multi-input, single-output compensator including all group sensors as inputs and the local actuator as an output. Note that some nodes belong to more than one group and, therefore, contribute to more than one compensator.

## Experimental Results

In this section, the control performance of various distributed architectures is compared. The primary metric used to evaluate system performance is the transfer function from the disturbance to sensor outputs in the closed-loop system. Note that the system $H_2$-norm between the disturbance input and all control signal outputs was checked for each system to ensure that the control effort was equal for all global systems. This provided for a fair comparison between different architectures.

**Geographic group control performance**

As described previously, geographic groups consist of sensors in physical proximity to each other.

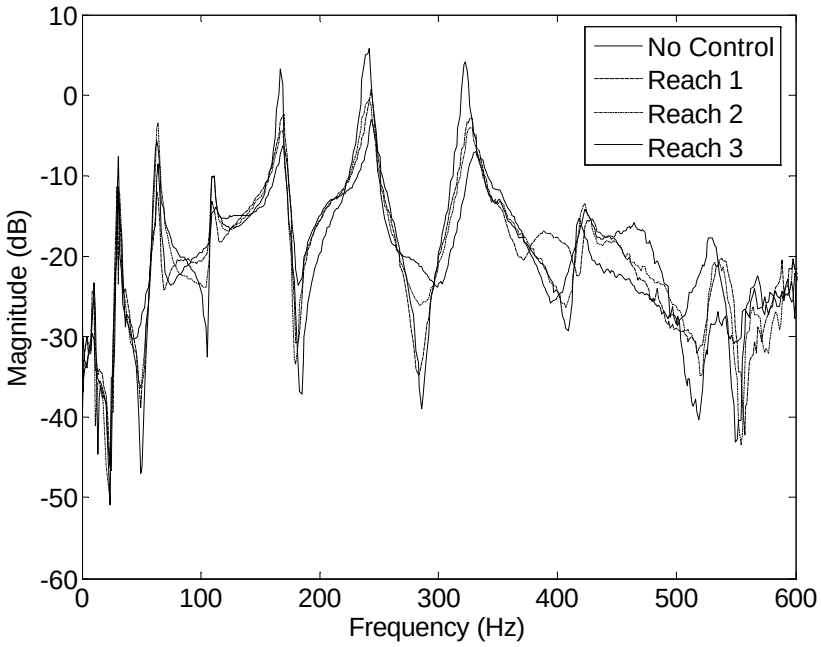


**Figure 4-7**. Transfer functions of distributed systems with reach 1, 2 and 3.

The transfer function plots are shown in Figure 4-7 for the open loop system and distributed control systems with reach 1, 2 and 3 (i.e. group sizes of 1, 5 and 6 sensors). As shown in Figure 4-7, all distributed systems achieve good vibration reductions, especially on the three dominant vibrational modes: 165.4Hz, 235.8Hz and 318.9Hz. Furthermore, as one would expect, the control performance improves when the reach is increased.

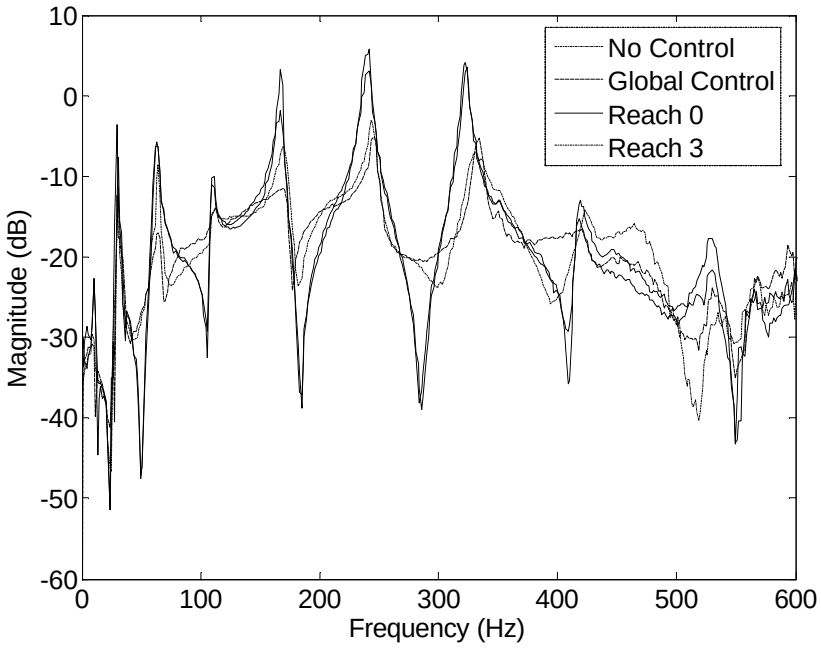


**Figure 4-8**. Transfer functions of centralized and distributed control systems.

As the reach increased, the distributed control architecture approaches the centralized control system since each compensator has most (if not all in the case of some controllers with reach 3) of the system sensor signals available. One would, therefore, expect that the performance of distributed control would approach that of centralized systems. This is demonstrated in Figure 4-8. As shown in Figure 4-8, the distributed control system of reach 3 approaches the performance of a centralized control system at the three dominant vibrational modes. A tentative conclusion based on this result (and supported by previous work[9]) is that, as the reach of a geographic distributed controller increases and the available sensor signals span a significant amount of the structures length, the performance of the distributed control system will approach that of a centralized controller. This result can be achieved without including all system sensor signals, but only enough to span a significant portion of the length[9].

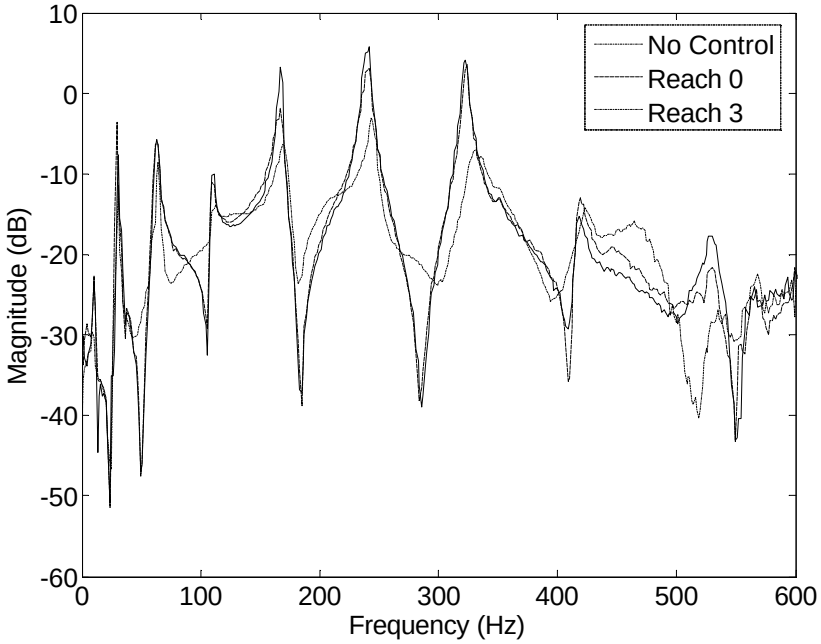


**Figure 4-9**. Transfer functions of decentralized and distributed control systems.

A last comparison is provided in Figure 4-9 which shows the performance of a distributed controller of reach 3 with a controller of reach 0. A reach zero controller is equivalent to a decentralized controller since it only utilizes the local sensor signal to create the local control signal. As demonstrated by Figure 4-9 distributed control significantly outperforms the decentralized compensator at the three dominant vibration frequencies. Vibrational modes at the lower frequency range are also reduced further when compared to decentralized control system. The advantage of a purely decentralized control system is that it is infinitely scalable. That is to say, as the number of system sensors increases there is no increase in controller complexity since there is no communication among separate localized controllers. However, the advantage of a distributed controller is that it's performance is better than decentralized, but at the cost

of added complexity both in terms of signal communications and controller complexity. But, when applied to a large scale system, the trade off between performance and complexity offered by a distributed system (as compared to either decentralized or centralized) offers system designers some choices.

**Modal group control performance**

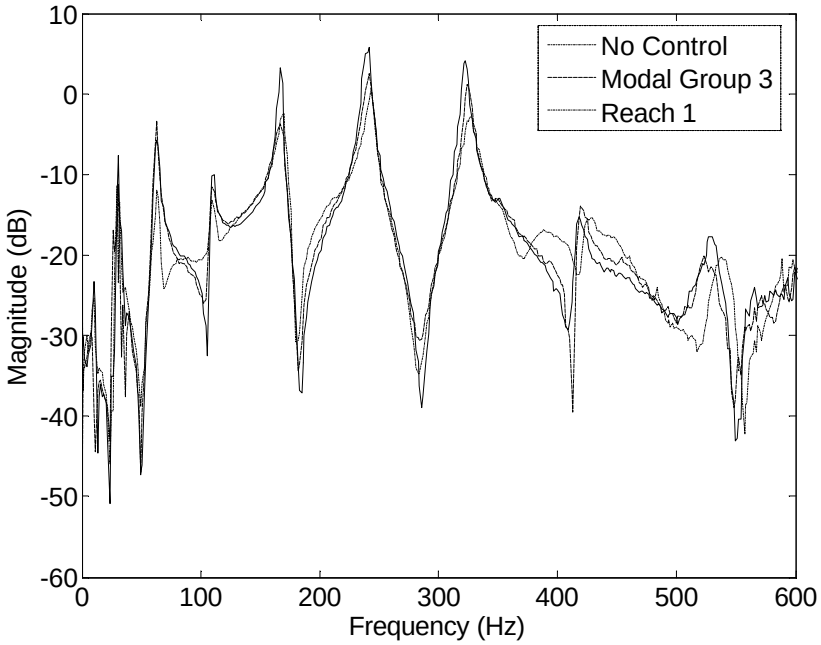


**Figure 4-10**. Transfer functions of distributed control based on modal groups with 3 members.

The performance of controllers using groups based on modal sensitivity is shown in Figure 4-10 as compared to the reach 1 geographic group architecture. While the modal group architecture is able to significantly attenuate the three target modes, it achieves less attenuation than the reach 1 geographic architecture. Both of these architectures employ groups with 3 members each. A similar result was noted based on

computer simulations[9]. This result is unexpected since modal based control systems have proven effective in previous investigations. It may be true that with larger group sizes and optimized sensor grouping, that this trend would not continue.

**Table 4-4**. Overall vibration reductions for different control architectures

| Control Architecture | Overall Vibration Power |
|---|---|
| Open loop | 0.6416 |
| Global control | 0.3039 |
| Local control reach = 0 | 0.5745 |
| Geographic, reach = 1 | 0.4724 |
| Geographic, reach = 2 | 0..4434 |
| Geographic, reach = 3 | 0.3707 |
| Modal, 3 members | 0.5063 |

A final comparison of all control architecture's overall performance is provided in Table 4-4, which shows the total $H_2$-norm between the disturbance input and all sensor outputs. Note that, as stated previously, centralized control offers the best performance overall. However, among distributed control architectures the geographic groups offer the best performance when compared to the modal groups.

## Conclusions

In this paper distributed control systems with different architectures have been investigated experimentally to reduce the vibration of a simply supported beam. Distributed control with geographic and modal grouping have been studied. The design

of a distributed controller based on $H_2$ optimal control technique was described, and experiments were done to compare the performances of different control architectures. It is shown that distributed control has a better performance than decentralized control, and the performance can be improved by increasing the reach or number of sensors in a group. Experimental results demonstrate that the distributed control method approaches the performance of a traditional centralized controller when as the size of the group is increased. A further advantage of these group-based architectures is that they are scalable for use in large scale systems, similar to the decentralized design.

## Acknowledgements

This work was supported by the DARPA Information Exploitation Offices' Network Embedded System Technology (NEST) Program and a National Science Foundation CAREER Award No. CMS-0134224.

## References

[1] W. T. Baumann, W. R. Saunders, and H. H. Robertshaw, "Active suppression of acoustic radiation from impulsively excited structures," Journal of the Acoustical Society of America, Vol. 90, No. 6, 1991, pp. 3202-3208.

[2] R. L. Clark and C. R. Fuller, "Control of sound radiation with adaptive structures," Journal of Intelligent Material Systems and Structures, Vol. 2, No. 3, 1991, pp. 431-452.

[3] R. L. Clark, W. R. Saunders, and G. P. Gibbs, *Adaptive Structures: Dynamics and Control*, Wiley, New York, 1998.

[4] C. R. Fuller, "Experiments on reduction of aircraft interior noise using active control of fuselage vibration," Journal of the Acoustical Society of America, Vol. 78, No. S1, 1985, pp. S88.

[5] L. Meirovitch, *Dynamics and Control of Structures,* wiley-Interscience, March 1990.

[6] C. Y. Chong and S. P. Kumar, "Sensor networks: evolution, opportunities, and challenges," Proceedings of the IEEE, Vol. 91, No. 8, 2003, pp. 1247-1256.

[7] S. Burke and J. Hubbard, Jr., "Active vibration control of a simply supported beam using a spatially distributed actuator," IEEE Control Systems Magazine, Vol. 7, No. 4, 1987, pp. 25-30.

[8] R. S. Chandra, J. Fowler, and R. D'Andrea, "Control of interconnected systems of finite spatial extent," IEEE Conference on Decision and Control, No., 2002, pp. 238-239.

[9] K. D. Frampton, "Distributed group-based vibration control with a networked embedded system," Smart Materials & Structures, Vol. 14, No. 2, 2005, pp. 307-314.

[10] B. Sinopoli, C. Sharp, L. Schenato, S. Schaffert, and S. S. Sastry, "Distributed control applications within sensor networks," Proceedings of the IEEE, Vol. 91, No. 8, 2003, pp. 1235-1246.

[11] E. Scholte and R. D'Andrea, "Active vibro-acoustic control of a flexible beam using distributed control," American Control Conference, Denver, CO, 2003.

[12] G. West-Vukovich, E. Davison, and P. Hughes, "The decentralized control of large flexible space structures," IEEE Transactions on Automatic Control, Vol. 29, No. 10, 1984, pp. 866-879.

[13] K. D. Frampton, "Decentralized control of structural acoustic radiation," Proceedings of IMECE 2000, New York, NY, 2001.

[14] M. Baudry, P. Micheau, and A. Berry, "Decentralized harmonic active vibration control of a flexible plate using piezoelectric actuator-sensor pairs," Journal of the Acoustical Society of America, Vol. 119, No. 1, 2006, pp. 262-277.

[15] O. N. Baumann, W. P. Engels, and S. J. Elliott, "A comparison of centralized and decentralized control for the reduction of kinetic energy and radiated sound power," Proceedings of Active04, Williamsburg, VA, 2004.

[16] M. J. Brennan, S. J. Elliott, and X. Huang, "A demonstration of active vibration isolation using decentralized velocity feedback control," Smart Materials & Structures, Vol. 15, No. 1, 2006, pp. N19-N22.

[17] W. P. Engels, O. N. Baumann, S. J. Elliott, and R. Fraanje, "Centralized and decentralized control of structural vibration and sound radiation," Journal of the Acoustical Society of America, Vol. 119, No. 3, 2006, pp. 1487-1495.

[18] P. Gardonio, E. Bianchi, and S. J. Elliott, "Smart panel with multiple decentralized units for the control of sound transmission. Part I: theoretical predictions," Journal of Sound and Vibration, Vol. 274, No. 1-2, 2004, pp. 163-192.

[19] P. Gardonio, E. Bianchi, and S. J. Elliott, "Smart panel with multiple decentralized units for the control of sound transmission. Part II: design of the decentralized control units," Journal of Sound and Vibration, Vol. 274, No. 1-2, 2004, pp. 193-213.

[20] N. A. Lynch, *Distributed Algorithms*, Morgan Kaufmann Publishers, 1996.

[21] D. C. Schmidt and S. D. Huston, *C++ Network Programming: Mastering Complexity Using ACE and Patterns*, Addison-Wesley Longman, 2002.

[22] R. Nagpal and D. Coore, "An algorithm for group formation in an amorphous computer," Proceedings of the 10th International Conference on Parallel and Distributed Computing Systems (PDCS'98), Nevada, October 1998.

[23] G.-C. Roman, Q. Huang, and A. Hazem, "Consistent group membership in ad hoc networks," Proceedings of the 23rd International Conference on Software Engineering (ICSE), 2001.

[24] R. Vitenberg, I. Keidar, and G. V. Chockler, "Group communication specifications: a comprehensive study," ACM Computing Surveys, Vol. 33, No. 4, December 2001, pp. 1-43.

[25] M. Maroti, K. D. Frampton, G. Karsai, S. Bartok, and A. Ledeczi, "Experimental platform for studying distributed embedded control applications," Proceedings of Languages, Compilers, and Tools for Embedded Systems Conference, Berlin, Germany, June 2002.

[26] T. Tao, K. D. Frampton, and A. Ledeczi, "Simulations of decentralized vibration control with a networked embedded system," Proceedings of SPIE Annual International Symposium on Smart Structures and Materials - The Internation Society for Optical Engineering, San Diego, CA, 2003.

[27] T. Tao and K. D. Frampton, "Distributed vibration control with sensor networks," Proceedings of SPIE Smart Structures and Materials 2006: Modeling, Signal Processing, and Control, San Diego, CA, 2006.

[28] J. C. Doyle, K. Glover, P. P. Khargonekar, and B. A. Francis, "State-space solutions to standard H2 and H∞ control problems," IEEE Transactions on Automatic Control, Vol. 34, No. 8, 1989, pp. 831-847.

[29] W. T. Thomson and M. D. Dahleh, T*heory of Vibration with Applications,* Prentice Hall, Upper Saddle River, NJ, 1998.

[30] K. Zhou, J. C. Doyle, and K. Glover, R*obust and Optimal Control,* Prentice-Hall, Upper Saddle River, NJ, 1995.

# CHAPTER V

## MANUSCRIPT 4

## FAULT-TOLERANT ACTIVE VIBRATION CONTROL FOR A SIMPLY SUPPORTED BEAM WITH HIGH ORDER

Tao Tao, Chakradhar Byreddy, and Kenneth D. Frampton

Vanderbilt University, Nashville, TN 37235, USA

(Submitted to Journal of Dynamic Systems, Measurement, and Control)

### Abstract

In this paper a fault-tolerant active vibration control system is applied to a simply supported beam with high order. System failures are detected and isolated by Beard-Jones (BJ) filters, and then a controller specifically designed for the faulty system is switched on, in order to maintain optimal control performance and stability under failure conditions. The BJ filters are designed based on system identification model for a simply supported beam. The controller library includes four controller designs which are used for different fault situations. The performance of a fault adaptive control system applicable to higher order systems are demonstrated experimentally, and the result provide a benchmark for the design of detection filters for use in fault-tolerant vibration control.

## Introduction

Active Control has been used to reduce structural vibrations for many years[1,2,3,4], and the application of active vibration control has been extended to large-scale systems[5,6,7,8]. Many control algorithms, such as adaptive feedback and adaptive feedforward controls, have been developed for different situations[9,10]. Since sensors and actuators are normally involved in such active control systems, the implementation of Fault Detection and Isolation (FDI) for sensor or actuator failures have been investigated for long-term safety[11,12,13,14,15]. However, no work has been done in fault-tolerant vibration control, since the high order vibration system limits the application of traditional fault-tolerant strategies.

The traditional fault detection work can be widely classified into four categories: 1. Algorithm based on Kalman filters; 2. Parity space techniques; 3. Diagnostic Observers; 4. Parameter estimation methods. The BJ filters are based on diagnostic observers, and have been demonstrated previously to offer several advantages in vibration control applications[11,12,16]. One of these advantages is that BJ filters utilize subspace concepts to associate the residual with the system faults, thereby permitting simultaneous FDI.

As described before, traditional fault detection algorithms including BJ filters are limited to relatively low order systems, since it is very difficult to obtain a BJ observer design that is stable when the system has high orders. However, the vibration systems, such as beams and plates, require large order models to ensure accuracy[5,17,18], which makes it hard to implement a fault toleration vibration control. Another limitation is that there are no existing design techniques than can accommodate a model with feed-through

dynamics (i.e. a state space model with non-zero D matrix). The vibration system models are normally obtained with system identification techniques, which usually result in models with feed-through dynamics[19,20,21].

In this work, the performance of a fault-tolerant active vibration control system is demonstrated experimentally. The fault tolerant method in this paper is based on BJ filters, and applicable for high order systems with feed-through dynamics. A simply supported beam with three pairs of piezoelectric transducers acting as sensors and actuators is the active structure investigated. The work presented here begins with a description of the experimental platform, followed by system identification results. Then, the design of fault-tolerant BJ filters applicable for high order systems are presented. Finally, the performance of the BJ filters and the fault-tolerant control system is demonstrated.

## Experimental Setup

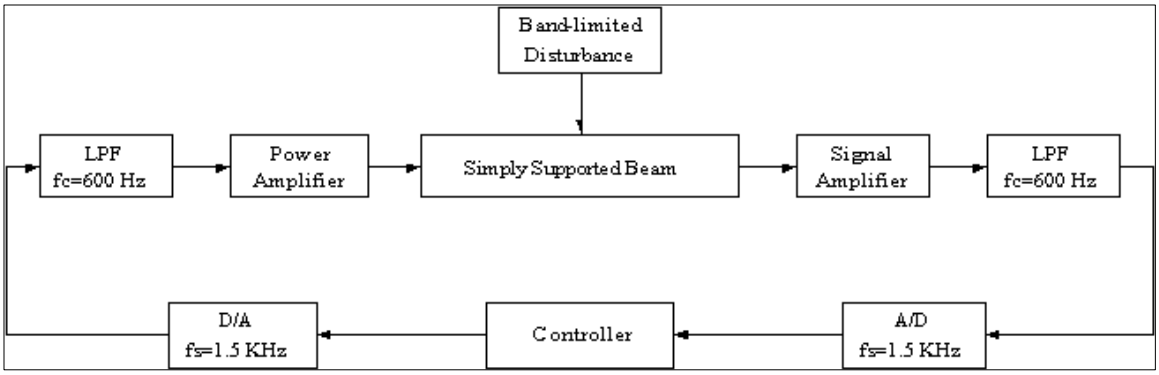


**Figure 5-1**. Block diagram of the experimental setup.

The instrumentation arrangement used in the experimental setup is shown schematically in Figure 5-1. The simply supported beam is disturbed by a band-limited white noise (0 - 600Hz) , and sensor signals are amplified and filtered with four-pole Butterworth low-pass filters. Distributed controllers are implemented on a dSPACE DS1103 PPC board, and control signals are amplified by a 790A06 power amplifier from PZB Piezotronics, Inc.

**Table 5-1**. Physical parameters of the experimental beam.

| Physical parameters | Values |
|---|---|
| Density | 2700 (kg/m3) |
| Thickness | 0.0032 (m) |
| Length | 1.0650 (m) |
| Width | 0.0508 (m) |
| Young's Modulus | 73.1E9 (Pa) |

The physical system is a beam made of aluminum 2024-T4, and the physical parameters are listed in Table 5-1.

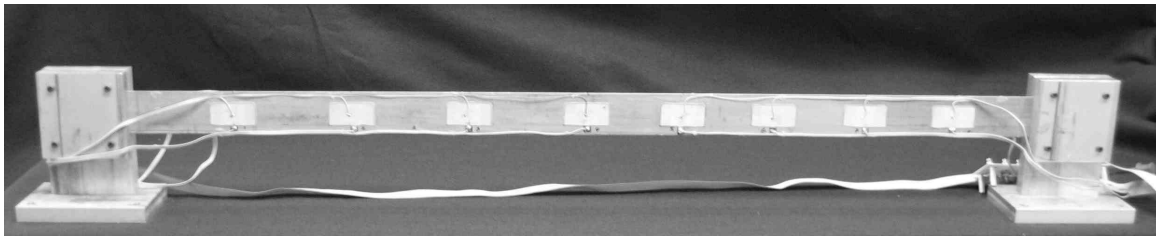

**Figure 5-2**. The experimental beam with multiple sensor/actuator pairs.

The beam is clamped at both ends, with grooves machined near both ends to approximate the simply supported boundary condition[18]. System identification results have shown that the beam's dynamic response is very close theoretical predictions for a simply supported beam.

Lead Zirconate Titanate (PZT) transducers are attached along the beam acting as sensors and actuators, as shown in Figure 5-2. The size of each PZT patch is 0.055m by 0.027m, and patches are not evenly distributed along the beam. All sensors are on the same side of the beam, and all actuators are on the opposite side. The band-limited noise is applied to PZT1 (left most transducer, with the coordinate 0.11m) as the disturbance. It is known that the transducer placements will affect control performance[19,22], and so the transducers were chosen to maximize sensitivity to the structural modes below 600 Hz. The three collocated pairs of transducers selected were: PZT2 (with a coordinate 0.26m) , PZT4 (with a coordinate 0.54m), and PZT7 (with a coordinate 0.87m) along the beam (as shown in Figure 5-2).

## System Identification

As specified previously, the system model obtained from theoretical derivation matches the experimental result well. However, since the control performance depends on the accuracy of the system model, the dynamics of the beam were obtained using experimental system identification.

Six sensors and six actuators were used for the control system, resulting in 36 transfer functions from the inputs to outputs. In addition, the path between disturbance and all sensors was also identified. A band-limited white noise was applied to each

actuator, and then all sensor and actuator data were collected to derive the Auto-Regression with eXtra inputs (ARX) model[21]:

$$y(t) + a_1 y(t-1) + \ldots + a_n y(t-n) = b_1 u(t-1) + \ldots + b_m u(t-m) \quad (1)$$

The ARX parameters were obtained using a batch least squares solution, and then a multi-input multi-output (MIMO) state-space model was derived from the corresponding ARX model.

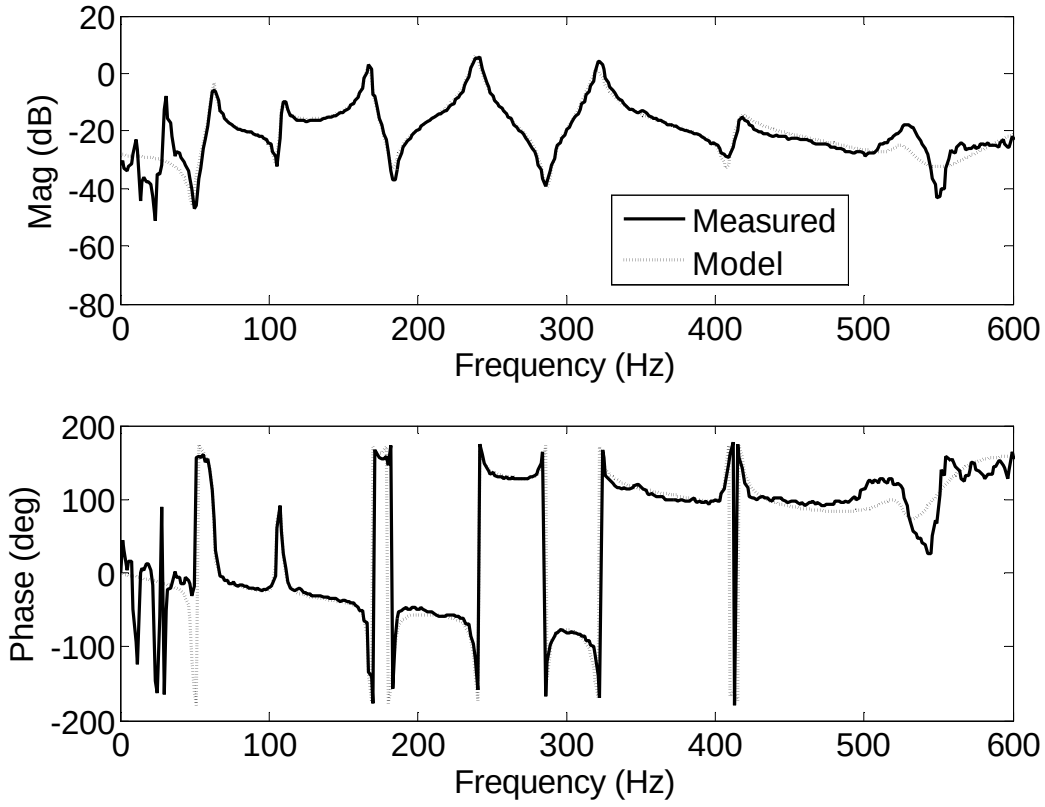


**Figure 5-3**. Experimental and analytical frequency responses from the disturbance to sensor 1.

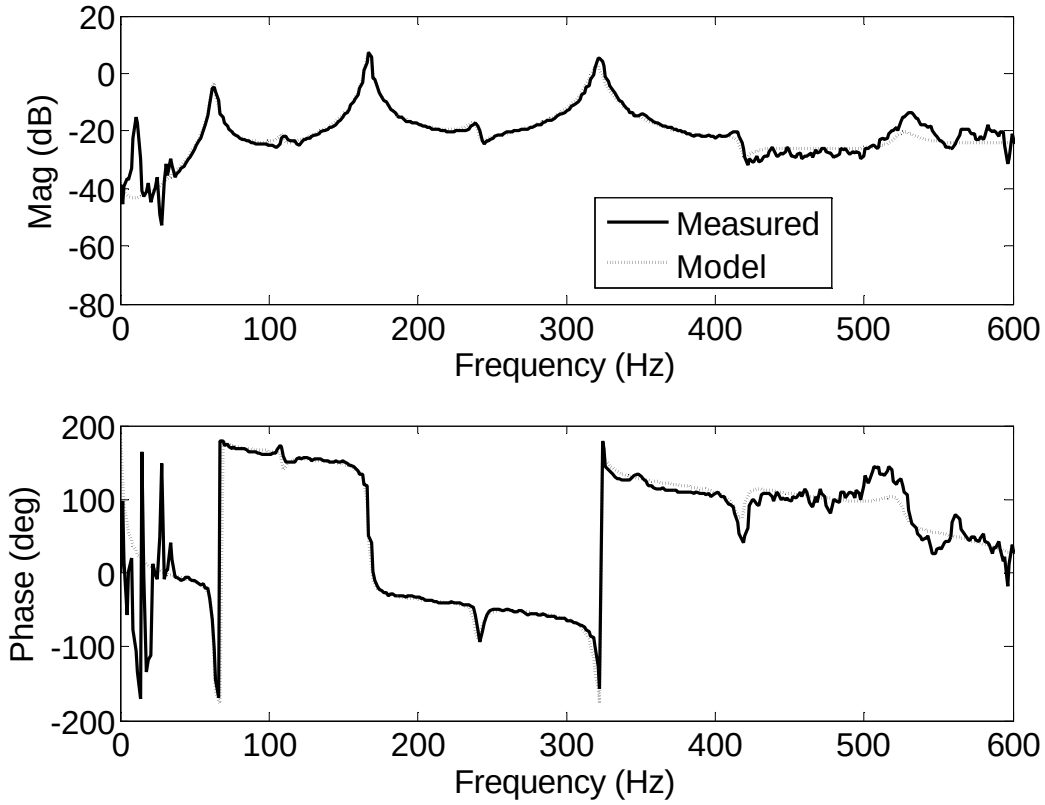


**Figure 5-4**. Experimental and analytical frequency responses from the disturbance to sensor 2.

The order of the system model in our experiment was chosen to be 36, and frequency responses of all signal paths match the experimental results very well. Experimental and analytical frequency responses of two signal paths are shown in Figures 5-3 and 5-4. In Figure 5-3, the solid lines represent the transfer function from the disturbance to sensor 1 measured directly from system identification data, while the dotted lines represent the derived state-space model with 36 states. It is clearly shown that the state-space model represent the beam dynamics very well, in both magnitude and phase of the system response. Similarly, the transfer function from the disturbance to

sensor 2, shown in Figure 5-4, demonstrates a good match between experimental and analytical responses. The other signal paths have similar results.

## BJ Detection Filter Theory and Design

BJ filters are a special case of the traditional Luyenberg observer. The difference is that for a BJ filter, the "free" parameters of the observer feedback matrix are selected in such a way that the output residual has specific directional properties when specific faults occur. Therefore, the residual can be monitored to both detect a fault, and isolate the specific fault, which has occurred. The basic theory of BJ filters is summarized in this section. This is followed by the development of two modifications to existing feedback matrix design techniques. The first modification enables BJ filters to be designed for systems with feed-through dynamics while the second modification presents a gain matrix design suitable for high order systems.

### The Traditional BJ Filter

BJ detection filters are traditional observers designed in such that the output residual vector has specific directional properties that can be associated with specific faults[14,23,24,25,26,27].

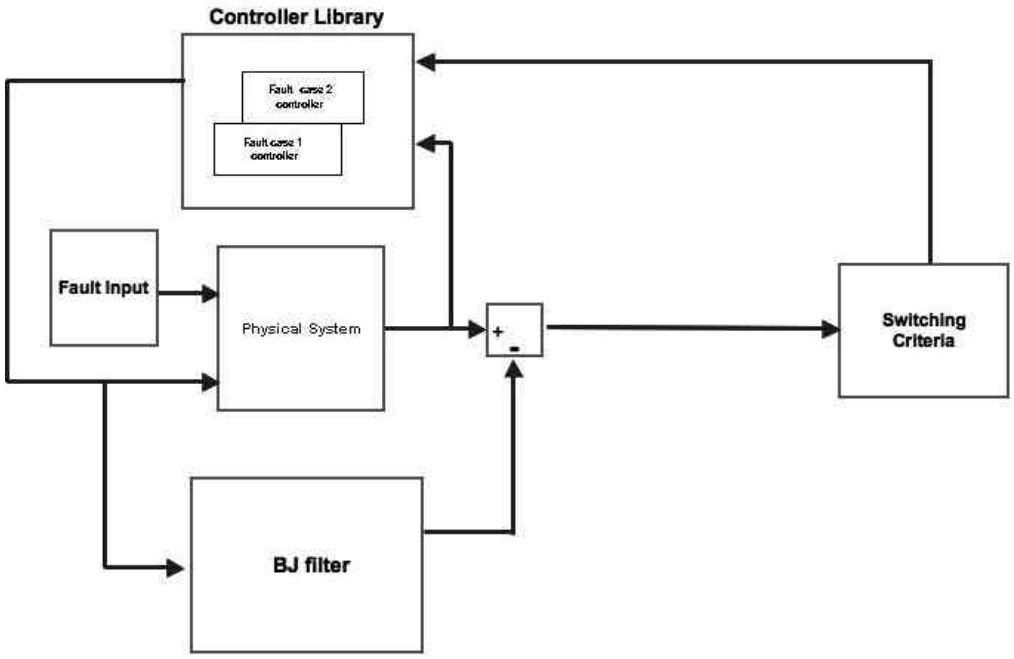


**Figure 5-5**: Basic model for Beard-Jones FDI.

The model for BJ FDI is shown in Figure 5-5. The BJ filter is of the form

$$\dot{\hat{\mathbf{x}}} = \mathbf{A}\hat{\mathbf{x}} + \mathbf{B}\mathbf{u} + \mathbf{L}(\mathbf{y} - \mathbf{C}\hat{\mathbf{x}}) \tag{2}$$

where $\hat{\mathbf{x}}$ is the state estimate and $\mathbf{L}$ is the detection gain matrix. The state error is as

$$\overset{\Delta}{e} = \mathbf{x} - \hat{\mathbf{x}} \tag{3}$$

Now the observer gain matrix $\mathbf{L}$ is chosen in such a way that the output error

$$\bar{e} = \mathbf{y} - \mathbf{C}\hat{\mathbf{x}} \tag{4}$$

has restricted directional properties in the presence of a failure. Therefore, when there are no faults present, the closed loop dynamics become

$$\dot{e} = \mathbf{G}e \tag{5}$$

where $\mathbf{G}$ is defined as

$$\mathbf{G} \overset{\Delta}{=} \mathbf{A} - \mathbf{L}\mathbf{C} \tag{6}$$

The presence of an additive fault, especially an actuator fault, can be modeled by adding a term to the open loop dynamic system obtained from system identification

$$\dot{\mathbf{x}} = \mathbf{A}\mathbf{x} + \mathbf{B}\mathbf{u} + \mathbf{f_i} m_i \tag{7}$$

where $\mathbf{f_i}$ is a nx1 design failure direction associated with the ith actuator failure and $m_i$ is a time-varying scalar which may be function of x(t) or u(t). Thus, the system output error in the presence of faults becomes

$$\begin{aligned} \dot{e} &= \mathbf{G}e + \mathbf{f_i} m_i \\ \bar{e} &= \mathbf{C}e \end{aligned} \tag{8}$$

The detection gain is designed in such a way that the directionality of the residual, $\bar{e}$, corresponds to specific faults. Design procedures are presented by Beard and Jones, and more recently by Kim et al.[14,23,24,25]. In this case, $\bar{e}$ is proportional to $\mathbf{C}\mathbf{f_i}$ in response to a failure corresponding to the direction $\mathbf{f_i}$.

**Design of BJ Filter with Feed-Through Dynamics**

It is not uncommon to encounter systems with feed-through dynamics (i.e. $\mathbf{D} \neq \mathbf{0}$), particularly when the working model results from model order reduction or system identification. However, there is as yet no way of dealing with this situation when designing BJ filters. This is because a potential actuator failure has a direct effect on the output of the system (which in turn can be interpreted to be a sensor failure). In order to avoid the confusion and isolate the actuator failure, a new BJ filter design method is presented for this particular case.

Consider a system with a non-zero $\mathbf{D}$ matrix. In addition to this consider a failure in actuator one. This particular case can be described

$$\begin{aligned}\dot{\mathbf{x}} &= \mathbf{A}\mathbf{x} + \mathbf{B}\mathbf{u} + \mathbf{b_1}du_1 \\ \mathbf{y} &= \mathbf{C}\mathbf{x} + \mathbf{D}\mathbf{u} + \mathbf{d_1}du_1\end{aligned} \tag{9}$$

where $\mathbf{b_1}$ and $\mathbf{d_1}$ are the first column vectors of **B** and **D** respectively, and $du_1$ represents the deviation of the first input caused by the failure in the actuator one. In order to develop a BJ filter it is assumed that $du_1$ behaves according to first order dynamics such that

$$\frac{ddu_1}{dt} = a\,du_1 + h \tag{10}$$

where $a$ and $h$ are constants. If the BJ theory fault is considered to be $m = du_1$, then Equations (9) and (10) can be combined in to a new state-space form

$$\begin{aligned}\begin{bmatrix}\dot{\mathbf{x}} \\ \dot{m}\end{bmatrix} &= \begin{bmatrix}\mathbf{A} & \mathbf{b_1} \\ 0 & a\end{bmatrix}\begin{bmatrix}\mathbf{x} \\ m\end{bmatrix} + \begin{bmatrix}\mathbf{B} \\ 0\end{bmatrix}u + \begin{bmatrix}0 \\ 1\end{bmatrix}h \\ \mathbf{y} &= \begin{bmatrix}\mathbf{C} & \mathbf{d_1}\end{bmatrix}\begin{bmatrix}\mathbf{x} \\ m\end{bmatrix} + \mathbf{D}\mathbf{u}\end{aligned} \tag{11}$$

Now, the usual BJ detection design outlined previously can be used on the appended system of Equation (11). It is possible that the appended system of Equation (11) may not meet all the requirements necessary to implement a BJ filter (i.e. observabilty and mutual detectability). In such a case other means must be employed to design or implement fault detection filters.

**Design of Detection Gain Matrix**

There are several gain selection methods available that work well for low order systems[11,13,15,28,29]. However, when the system order is large (greater than 10 or so), it is very difficult to use these methods and achieve a stable closed-loop detection filter.

In order to overcome this difficulty an unstable detection gain matrix is created using the invariant zero approach, and then modified to ensure a stable result. In most physical the detection orders are equal to one, which means that, for a given fault vector $\mathbf{f}$, the triplet (A, $\mathbf{f}$, C) has no invariant zero. In this case, the invariant zero approach yields a detection gain matrix $\mathbf{L}$ that is given by

$$\mathbf{L} = (\mathbf{AF} - \mathbf{F}\Delta)(\mathbf{CF})^{*} \tag{12}$$

where $\Delta$ is a diagonal matrix whose elements are given as the eigenvalues associated with the detection space of $\mathbf{F}$ and * indicates pseudo-inverse. Next, the result of equation (12) is modified to ensure a stable result according to the equation (13)

$$\mathbf{L}' = \mathbf{L} + \mathbf{E}(\mathbf{I} - (\mathbf{CF})(\mathbf{CF})^{*} \tag{13}$$

If the observer gain $\mathbf{L}'$ is applied to error state equation (5) then,

$$\mathbf{G} = (\mathbf{A} - \mathbf{L}'\mathbf{C}) = (\mathbf{A} - \mathbf{LC}) - \mathbf{E}(\mathbf{I} - (\mathbf{CF})(\mathbf{CF})^{*})\mathbf{C} \tag{14}$$

Now, if we define $\mathbf{A_f} = \mathbf{A} - \mathbf{LC}$ and $\mathbf{C_f} = [\mathbf{I} - (\mathbf{CF})(\mathbf{CF})^{*}]\mathbf{C}$, then $\mathbf{G} = \mathbf{A_f} - \mathbf{EC_f}$ and the dual of $\mathbf{G}$ is $(\mathbf{A_f^T} - \mathbf{C_f^T E^T})$. One will note that the definition of $\mathbf{G}$ is equivalent to the LQR control problem of finding an $\mathbf{E}$ that stabilizes $(\mathbf{A_f}, \mathbf{C_f})$ and minimizes

$$J = \sum \left[\mathbf{z^T Q z} + \mathbf{m^T R m} + 2\mathbf{z^T N m}\right] \tag{15}$$

where $\mathbf{z}$ and $\mathbf{m}$ are the states and inputs associated with the new pair $(\mathbf{A_f}, \mathbf{C_f})$. The weights $\mathbf{Q}$ and $\mathbf{R}$, can be altered to affect the closed-loop eigenvalues of the filter. It is assumed $\mathbf{N} = \mathbf{0}$ in these calculations. Finally, once a suitable matrix $\mathbf{E}$ is obtained the modified BJ filter gain matrix $\mathbf{L}'$ can be obtained from equation (13).

### Continuous/Discrete Residuals and Finite States

Where a fault is detected in the system, the physical system response deviates from that predicted by the BJ filter, resulting in a non-zero residual output from the filter called the continuous residual. When the continuous residual exceeds a pre-set threshold values, the corresponding entry in the discrete residual vector is set to one. If the continuous residual value falls below the threshold, the discrete vector is set to zero. This discrete residual vector is supplied to select the appropriate controller based on the fault case. One of the key features in the BJ filter is that it is able to detect multiple faults with a single filter; referred to as mutual detectability. Therefore, a single BJ filter is used to observe the system in any of the four fault modes. Not all systems are mutually detectable, however in systems where it is not; multiple BJ filters are designed and operated in parallel.

## Controller design

The distributed controllers in this work are designed based on H2 optimal control theory[30,31]. The approach used here is no different from traditional H2 control theory. But the arrangement and implantation in a distributed manner is unique. Such H2 optimal control has been proven effective and robust at attenuating structural vibration in centralized strategy, and it is extended here to a distributed architecture.

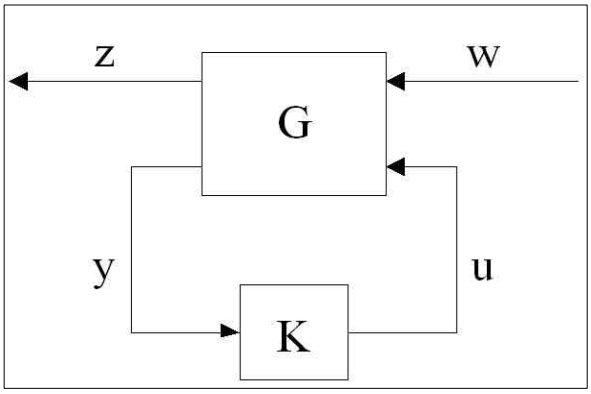


**Figure 5-6**. Basic H2 closed-loop system.

The basic block diagram of H2 closed-loop system is shown in Figure 5-6, where G is the generalized plant, K is desired controller, w is the exogenous input vector consisting of the disturbance and sensor noises, u is the control signal vector, and y is the plant output vector. In Figure 5-5, z is the output to be minimized which consists of the filtered actuator signals, system states and plant outputs. The goal of H2 optimal control is to compute an internally stabilizing controller K, which minimizes the transfer function $\|Tzw\|_2$. Details concerning the calculation of the optimal controller K can be found in reference[30,31].

In the control library, there are four controllers: controller for no fault, controller for actuator 1 failure, controller for actuator 2 failure, and controller for actuator 1 & 2 failure. All four controllers were designed based on H2 optimal control strategy.

## Experimental results

The failure of an actuator was implemented by unplugging the BNC cable from the Digital Analog Converter (DAC) on the dSPACE connection panel.

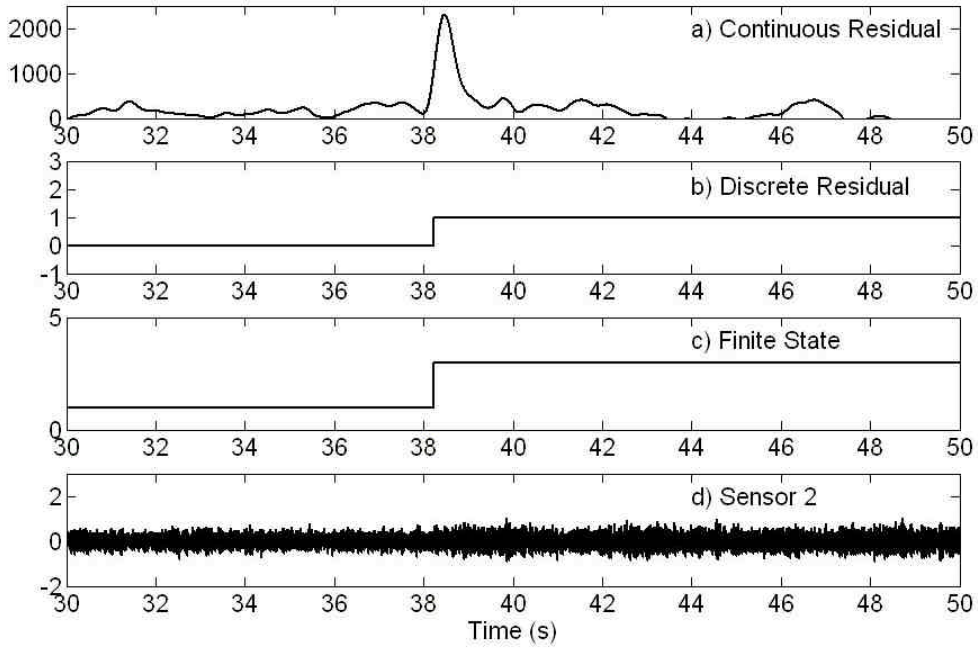


**Figure 5-7**. Time history of residuals and finite state for actuator 2 failure.

The time history of continuous residual, discrete residual, finite state and the output of sensor 2 were presented in Figure 5-7. It is shown that where there is a failure at actuator 2 around 38 seconds, the BJ filter detects the failure and the discrete residual is set to be 1 for actuator 2. The value of finite state is 3, which represents the failure of actuator 2 and switches the controller. Although the performance of the controller is a little worse after switch, the closed-loop system is stable and the transition between controller switch is negligible.

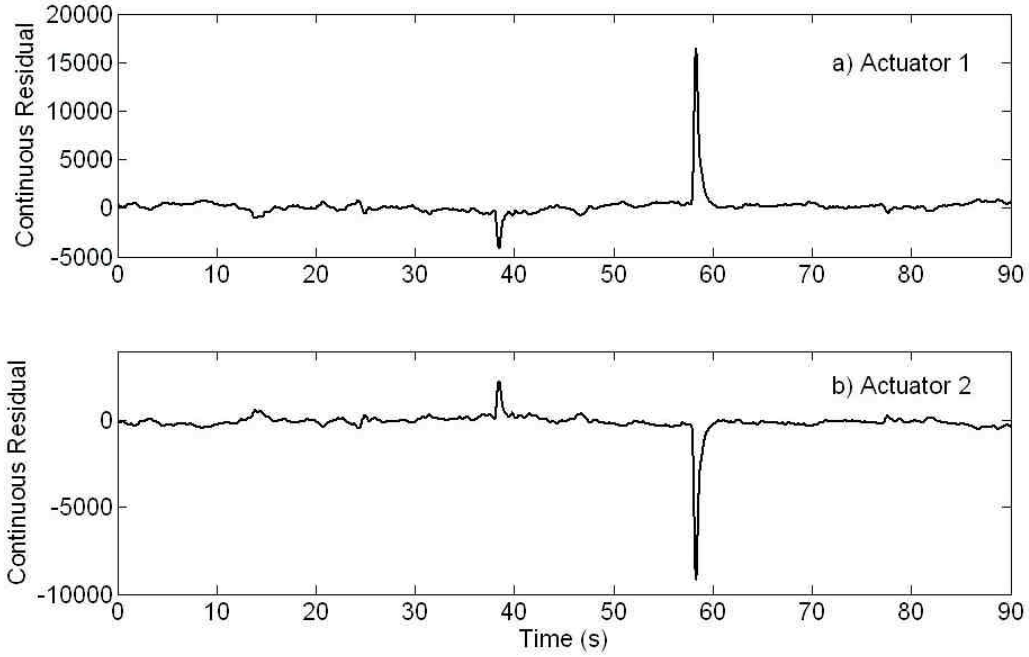


**Figure 5-8**. Continuous residuals for actuators 1 & 2 failures.

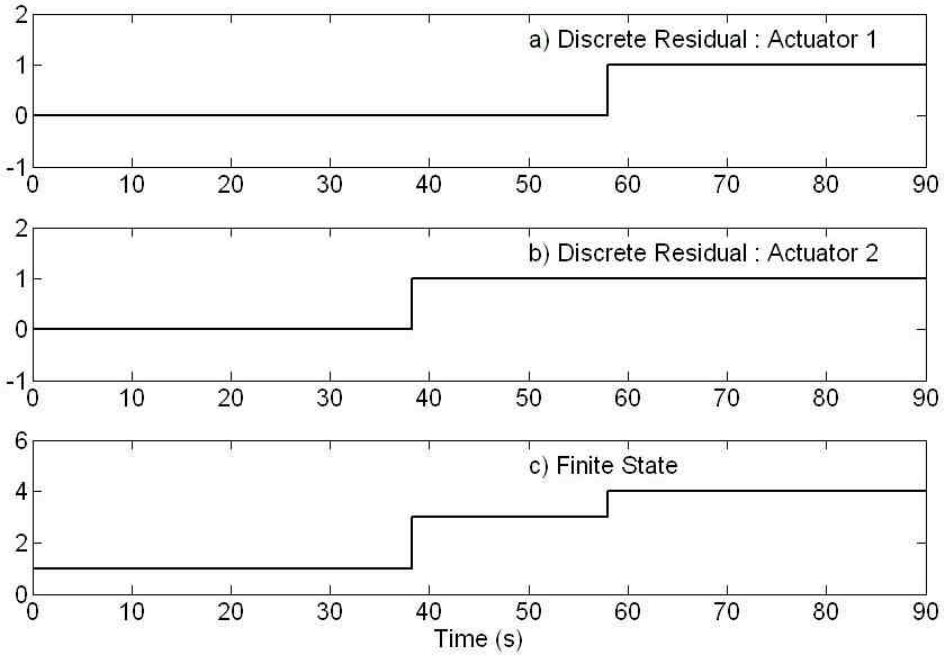


**Figure 5-9**. Discrete Residuals and finite state for actuators 1 & 2 failures

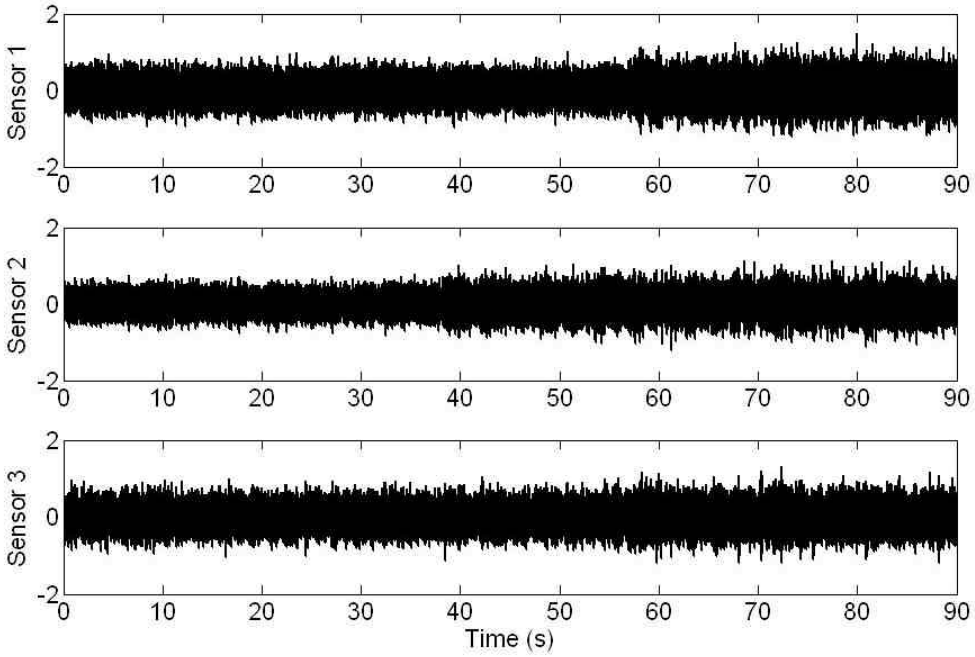


**Figure 5-10**. Sensor signals for actuator 1 & 2 failures.

The results of the experiment with two actuator failures are shown in Figures 5-8, 5-9 and 5-10. The failure of actuator 2 happened around 40 seconds, and the failure of actuator 1 took place around 60 seconds. The continuous residuals for both actuators are shown in Figure 5-8, and the BJ filter in our system detected both failures well. The discrete residuals and finite state for actuators 1 & 2 failures are shown in Figure 5-9. When actuator 2 failed around 40 seconds, the discrete residual for actuator 2 was changed to 1, and the finite state was set to be 3, which switched the controller to the specific one in the controller library. Then, when actuator 1 failed around 60 seconds, the discrete residual for actuator 1 was changed to 1, and the finite state was set to be 4 and the controller was switched again. The corresponding sensor signals are shown in Figure 5-10.

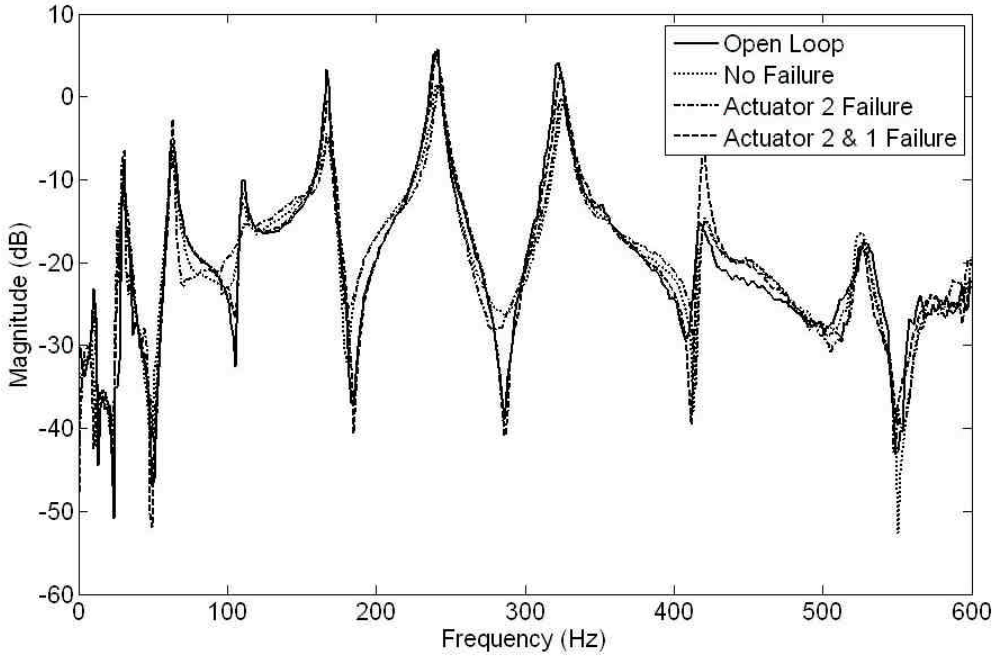


**Figure 11**. Transfer functions from the disturbance to sensor 1.

The transfer functions from the disturbance to sensor 1 in different fault situations are shown in Figure 5-11. It is shown that the system with no actuator failures has the best control performance, but the closed-loop system in our system is stable and fault-tolerant, even the control performance is compromised.

## Conclusions

In this work the fault-tolerant active vibration control system is implemented experimentally. The method is demonstrated applicable high order systems, such as the vibrational system with 36 states.

**Acknowledgements**

This work was supported by the DARPA Information Exploitation Offices' Network Embedded System Technology (NEST) Program and a National Science Foundation CAREER Award No. CMS-0134224.

**References**

[1] C. R. Fuller, "Experiments on reduction of aircraft interior noise using active control of fuselage vibration," Journal of the Acoustical Society of America, Vol. 78, No. S1, 1985, pp. S88.

[2] S. Burke and J. Hubbard, Jr., "Active vibration control of a simply supported beam using a spatially distributed actuator," IEEE Control Systems Magazine, Vol. 7, No. 4, 1987, pp. 25-30.

[3] W. T. Baumann, W. R. Saunders, and H. H. Robertshaw, "Active suppression of acoustic radiation from impulsively excited structures," Journal of the Acoustical Society of America, Vol. 90, No. 6, 1991, pp. 3202-3208.

[4] R. L. Clark and D. E. Cox, "Multi-variable structural acoustic control with static compensation," Journal of the Acoustical Society of America, Vol. 102, No. 5, 1997, pp. 2747-2756.

[5] O. N. Baumann, W. P. Engels, and S. J. Elliott, "A comparison of centralized and decentralized control for the reduction of kinetic energy and radiated sound power," Proceedings of Active04, Williamsburg, VA, 2004.

[6] M. J. Brennan, S. J. Elliott, and X. Huang, "A demonstration of active vibration isolation using decentralized velocity feedback control," Smart Materials & Structures, Vol. 15, No. 1, 2006, pp. N19-N22.

[7] K. D. Frampton, "Distributed group-based vibration control with a networked embedded system," Smart Materials & Structures, Vol. 14, No. 2, 2005, pp. 307-314.

[8] G. West-Vukovich, E. Davison, and P. Hughes, "The decentralized control of large flexible space structures," IEEE Transactions on Automatic Control, Vol. 29, No. 10, 1984, pp. 866-879.

[9] W. T. Baumann, "An adaptive feedback approach to structural vibration suppression," Journal of Sound and Vibration, Vol. 205, No. 1, 1997, pp. 121-133.

[10] S. C. Douglas, "Fast implementations of the filtered-X LMS and LMS algorithms for multichannel active noise control," IEEE Transactions on Speech and Audio Processing, Vol. 7, No. 4, 1999, pp. 454-465.

[11] H. Jones, "Failure detection in linear systems," The Charles Stark Draper Laboratory, Cambridge, MA Report No. T-608, 1973.

[12] R. V. Beard, "Failure accommodation in linear systems through self-reorganization," in *Aeronautics and Astronautics*. MA: Massachusetts Institute of Technology, 1971.

[13] J. Chen, R. J. Patton, and H. Y. Zhang, "Design of unknown input observers and robust fault detection filters," International Journal of Control, Vol. 63, No. 1, 1996, pp. 85-105.

[14] Y. Kim and J. Park, "An analysis of detection spaces using invariant zeros," American Control Conference, San Diego, CA, USA, 1999.

[15] R. Scattolini and N. Cattane, "Detection of sensor faults in a large flexible structure," Iee Proceedings-Control Theory and Applications, Vol. 146, No. 5, 1999, pp. 383-388.

[16] C. Byreddy and K. D. Frampton, "Simulations of fault-adaptive vibration control," ASME International Mechanical Engineering Congress and Exposition, Floria, 2005.

[17] W. J. Manning, A. R. Plummer, and M. C. Levesley, "Vibration control of a flexible beam with integrated actuators and sensors," Smart Materials & Structures, Vol. 9, No. 6, 2000, pp. 932-939.

[18] W. T. Thomson and M. D. Dahleh, *Theory of Vibration with Applications*, Prentice Hall, Upper Saddle River, NJ, 1998.

[19] R. L. Clark, W. R. Saunders, and G. P. Gibbs, *Adaptive Structures: Dynamics and Control*, Wiley, New York, 1998.

[20] J.-N. Juang, *Applied System Identification*, Prentice Hall, Englewood Cliffs, NJ, 1994.

[21] L. Ljung, *System Identification: Theory for the User*, Prentice Hall, Upper Saddle River, NJ, 1998.

[22] D. Halim and S. O. R. Moheimani, "An optimization approach to optimal placement of collocated piezoelectric actuators and sensors on a thin plate," Mechatronics, Vol. 13, No. 1, 2003, pp. 27-47.

[23] Y. Kim and J. Park, "A condition of the eigenvalues of detection filters for disturbance attenuation: an invariant zero approach," Conference on Decision and Control (CDC), Hawaii, USA, 2003.

[24] Y. Kim and J. Park, "Noise response of detection filters: relation between detection space and completion space," Iee Proceedings-Control Theory and Applications, Vol. 150, No. 4, 2003, pp. 443-447.

[25] Y. Kim and J. Park, "On the approximation of fault directions for mutual detectabilty: An invariant zero approach," Ieee Transactions on Automatic Control, Vol. 50, No. 6, 2005, pp. 851-855.

[26] J. Park and G. Rizzoni, "An Eigenstructure Assignment Algorithm for the Design of Fault-Detection Filters," Ieee Transactions on Automatic Control, Vol. 39, No. 7, 1994, pp. 1521-1524.

[27] J. E. White and J. L. Speyer, "Detection Filter Design - Spectral Theory and Algorithms," Ieee Transactions on Automatic Control, Vol. 32, No. 7, 1987, pp. 593-603.

[28] R. K. Douglas and J. L. Speyer, "Robust fault detection filter design," Journal of Guidance Control and Dynamics, Vol. 19, No. 1, 1996, pp. 214-218.

[29] G. Rizzoni and P. S. Min, "Detection of Sensor Failures in Automotive Engines," Ieee Transactions on Vehicular Technology, Vol. 40, No. 2, 1991, pp. 487-500.

[30] K. Zhou, J. C. Doyle, and K. Glover, *Robust and Optimal Control*, Prentice-Hall, Upper Saddle River, NJ, 1995.

[31] J. C. Doyle, K. Glover, P. P. Khargonekar, and B. A. Francis, "State-space solutions to standard H2 and H∞ control problems," IEEE Transactions on Automatic Control, Vol. 34, No. 8, 1989, pp. 831-847.

# CHAPTER VI

# CONCLUSIONS

This work is the first experiment implemented in the distributed vibration control field, and control performance results demonstrate the effectiveness of the two distributed grouping approaches. A simply supported beam with six pairs of piezoelectric transducers acting as sensors and actuators is the active structure investigated. The disturbance on the beam is band-limited white noise (0 - 600 Hz). The dynamics of the beam are obtained using experimental system identification, and a 36 state model is selected for control design use after exploring various model sizes. Since existing distributed control design approaches are not applicable to structural vibration systems due to the strongly connected nature of vibration system dynamics, new distributed controllers are designed based on traditional $H_2$ optimal control theory. Such $H_2$ optimal control has been proven effective and robust at attenuating structural vibration in centralized strategy, and it is extended here to a distributed architecture. Two types of sensor grouping strategies in the distributed control system are considered: groups based on physical proximity and groups based on modal sensitivity. Distributed middleware services such as clock synchronization and network communications routing are also investigated and implemented experimentally for vibration control.